
*Long-term Observations in Geophysics from Subsurface to Space:*
*Instrumentation, Methods, Discoveries*

# The geomagnetic field:
# A signal for probing processes from the Earth's core to outer space

Hermann Lühr und Martin Rother

*Deutsches GeoForschungsZentrum GFZ, Sekt. 2.3, Geomagnetismus, Potsdam*

DGG-Plenarvortrag S2
München, 7 March 2022

## *The geomagnetic field*

To first order the geomagnetic field is similar to that of a dipole at Earth's center.

The main part is generated in the liquid outer core. On its way through the Earth mantle it provides interesting information about the interior.

One important feature, the geomagnetic field shields us from dangerous radiation coming from space.

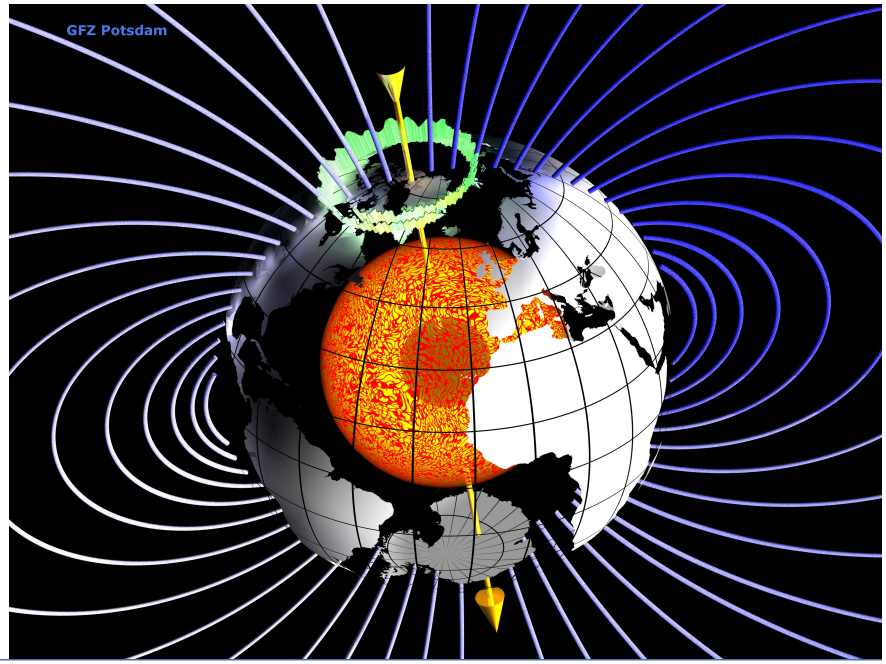

## *Outline*

- Journey through temporal and spatial scales
- Geomagnetic field modelling approaches
- Role of magnetic field for remote sensing
- Sensing electric currents in space
- Outlook

References

## *Characteristics of the geodynamo*

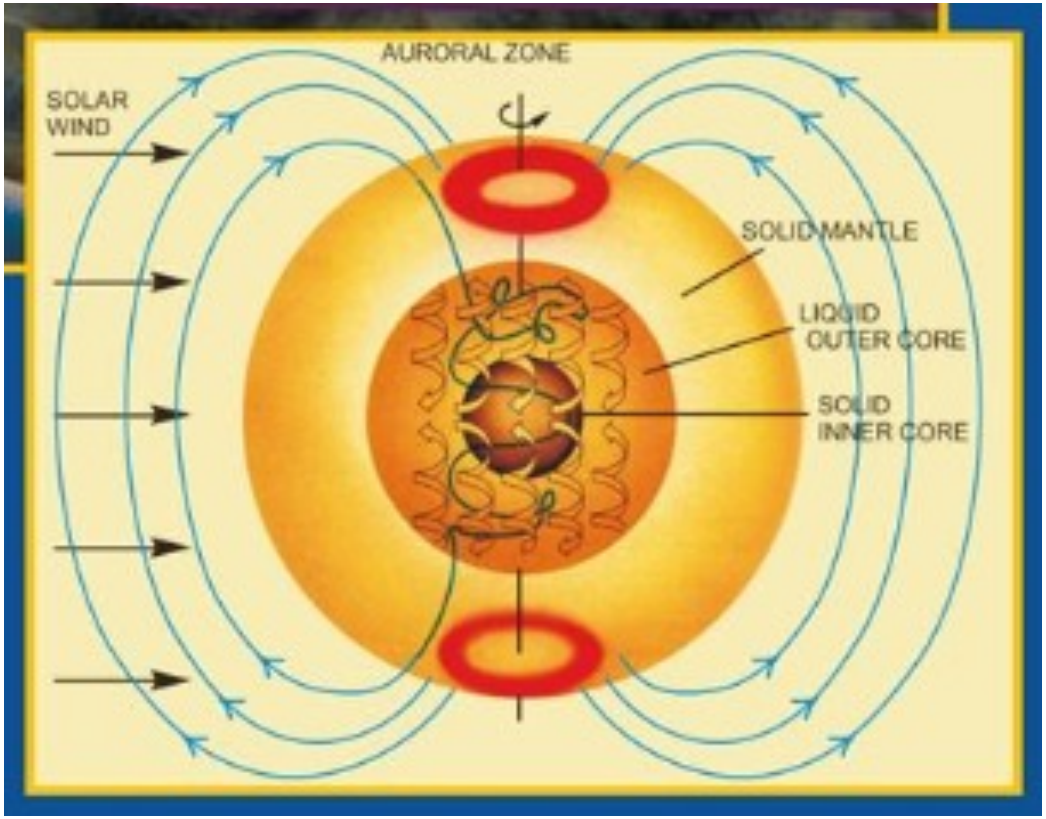


The geodynamo is driven by a thermal engine. The hot inner core drives convection motion within the above lying fluid iron. Due to Earth's rotation the material moves in spirals from the equator towards polar regions. Large parts of the geomagnetic field are generated in these flux bundles.

The generation process is constantly changing in an unpredictable chaotic way. At certain times even full polarity changes of the geomagnetic field occur.

During times of reversals the field strength is low, causing a much reduced shielding effect.

We will address field variations from long towards shorter time scales.

## *Series of geomagnetic field reversals*

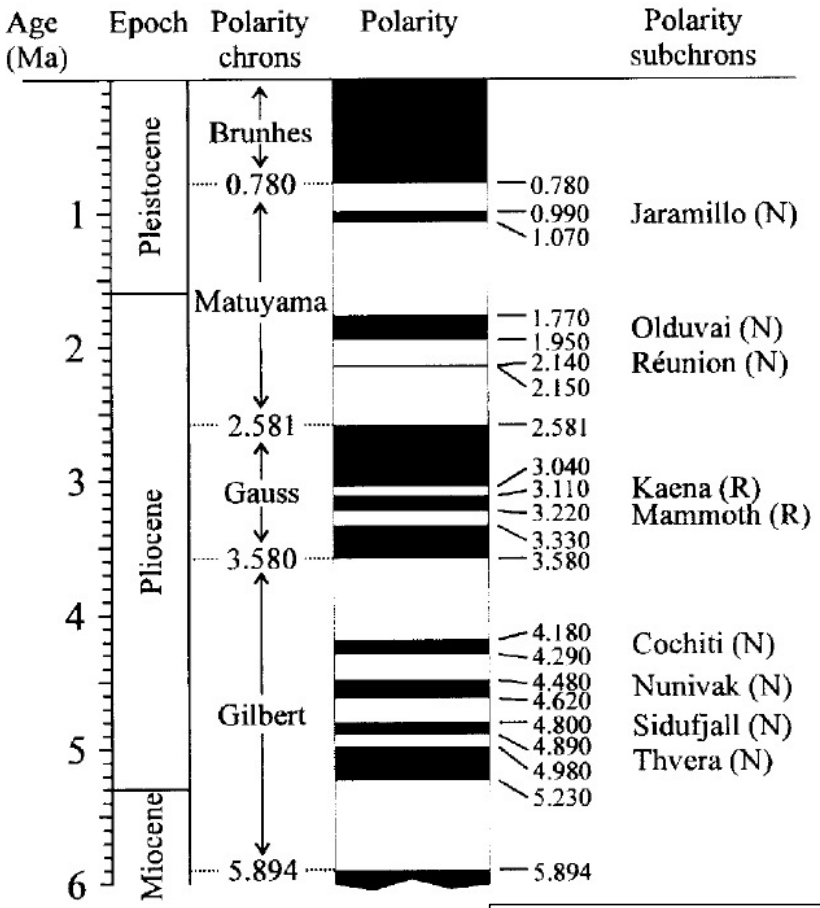


Cande and Kent (1995)

Rocks and sediments are wonderful archives that have stored past geomagnetic field directions. As soon as the material has cooled below the Curie temperature, it preserves the ambient field.
This allows to date the field direction changes.

Black, marks the normal field direction.

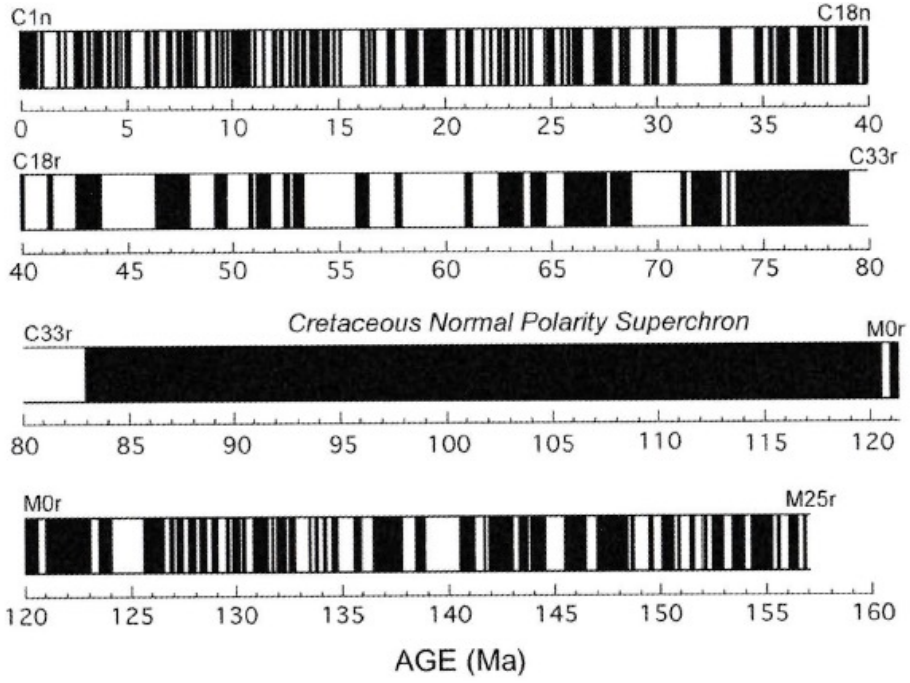

## *Geomagnetic excursions, definition*

In between full field reversals shorter-term field variations are observed.
These are termed excursions.

**Characteristics of geomagnetic excursions:** (definition varies)

- Large field direction variation, e.g. of the virtual geomagnetic pole (VGP) by more than 45° in latitude.
- Significant reduction in field strength, <25%
- Globally rather then locally observed effects.

## *Recent field excursions, Laschamp event*

Guyodo and Valet identified as part of their Sint-800 model a number of excursions within the recent Brunhes phase.

They use the field strength as threshold level for identifying excursions.

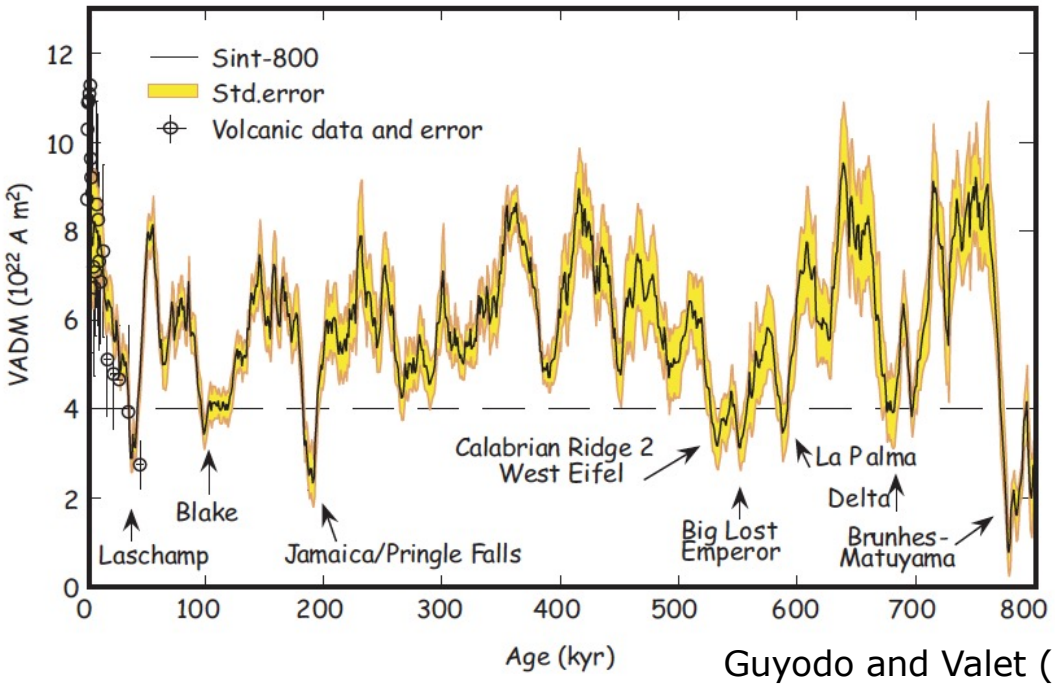


Guyodo and Valet (1999)

Particularly well studied is the recent Laschamp event occurring 40,000 years ago

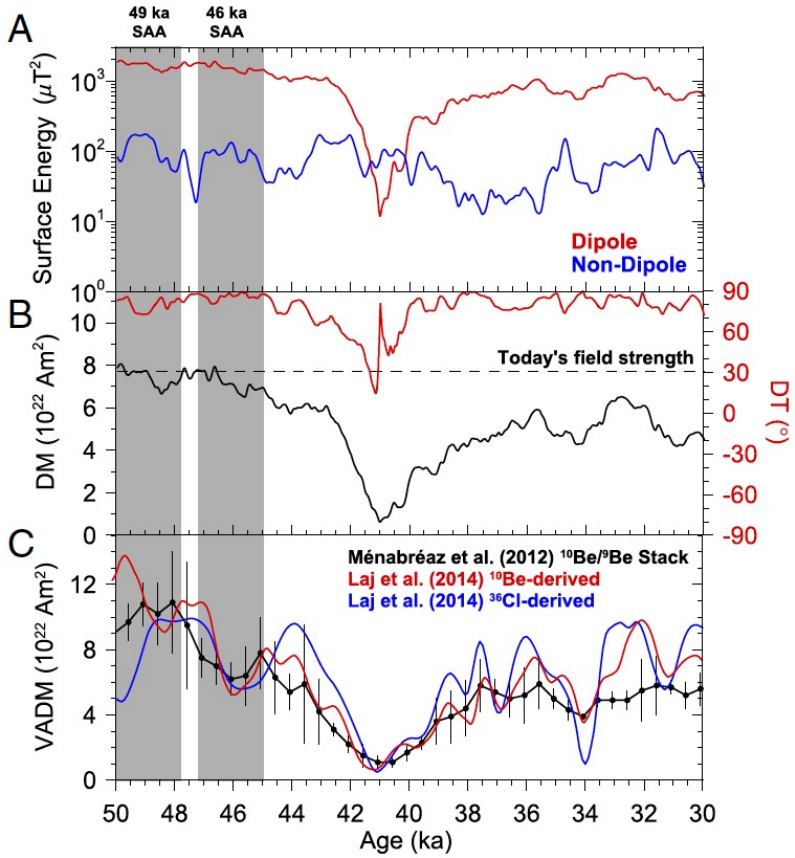


Brown et al. (2018)

## *Archeo-magnetic models of the past 10,000 years*

For the more recent past artefacts, pottery, and ice samples act as archives for the magnetic field reconstruction.
Quite reliable estimates of the field evolution during the past 10,000 years are obtained.

The field strength peaked around Anno Domini, about 40% higher than today. Since then it drops, until today.

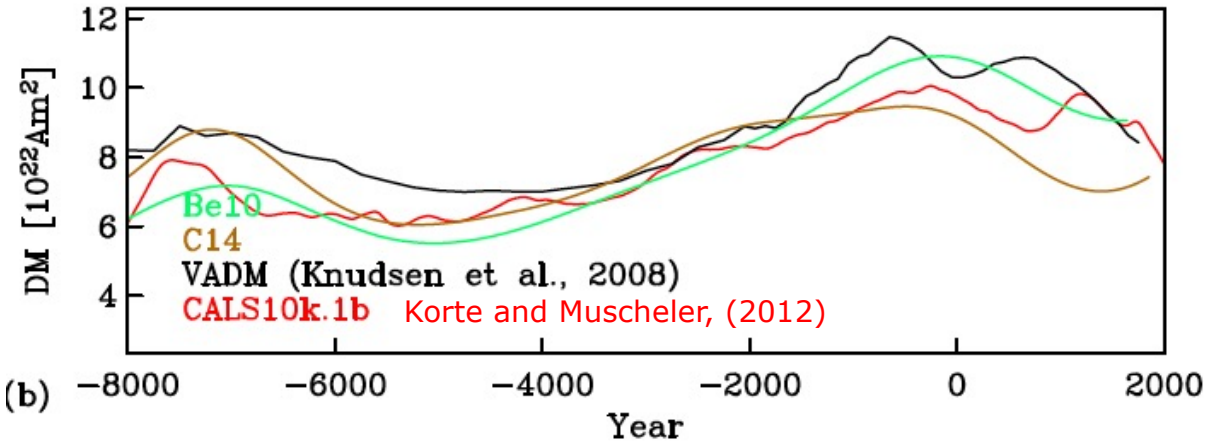


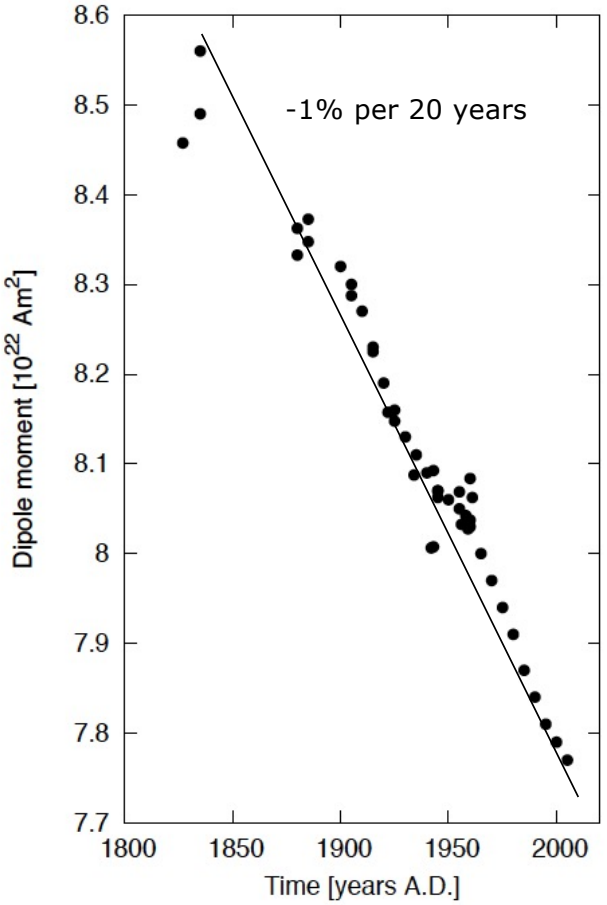

## *Why is it interesting to know the geomagnetic field?*

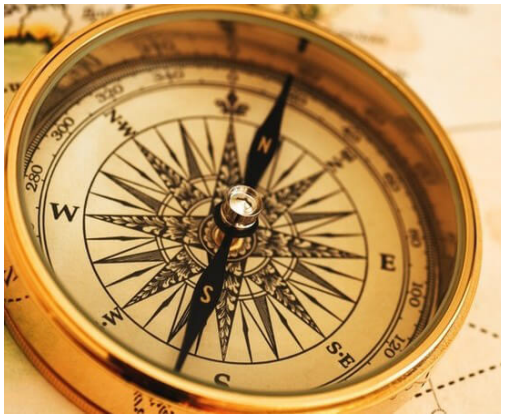

In the past the field direction was important for navigation.
Lots of efforts have been spent in mapping of the field. But soon it became evident that the field is changing with time.

Edmond Halley, ~1700

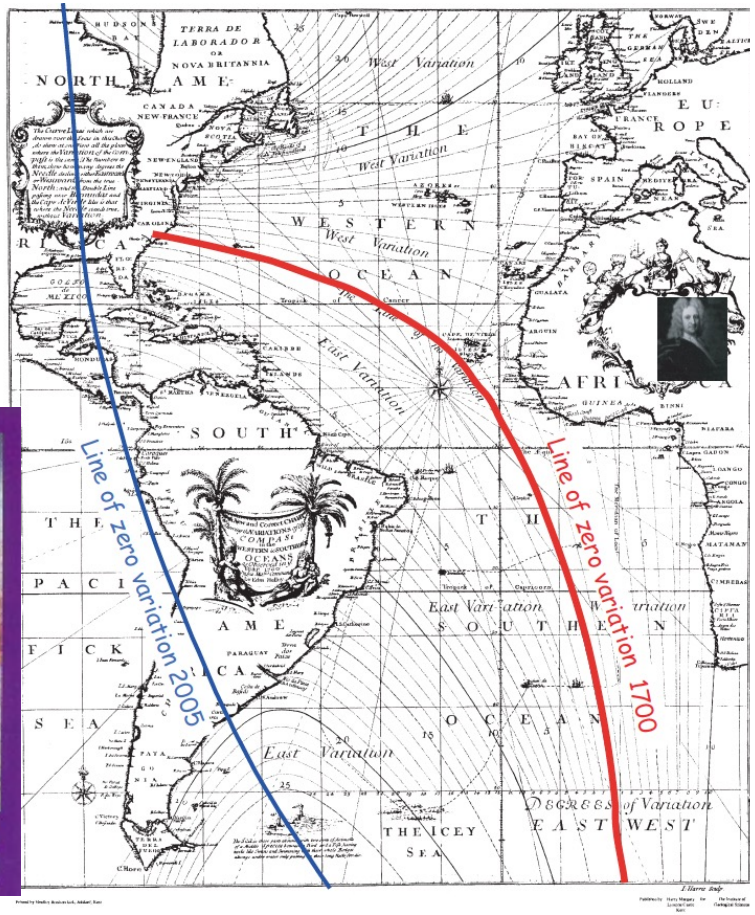


6 *Les premieres Ouevres de Iacques de Vaulx, pilotte en la Marine, Havre de Grace 1583.* Three methods of determining declination: at sunrise, at noon and at sunset. The central observer has an astrolabe, to ensure that the Sun has reached its highest point. (Courtesy of Bibliotheque Nationale, Paris; ms. inv. FR 150.)

## *C. F. Gauß, two seminal innovations for geomagnetism*

1) Carl-Friedrich Gauß invented a technique for absolute calibration of magnetic variometers and defined a common time bases for the global measurements (Göttinger Zeit).

2) He maded use of spherical harmonic function expansions, assuming that the geomagnetic field can be treated as a scalar potential field.

The magnetic field components result from the negative gradient of the potential.

In 1840 Gauß is the first to present a map of the global geomagnetic field distribution.

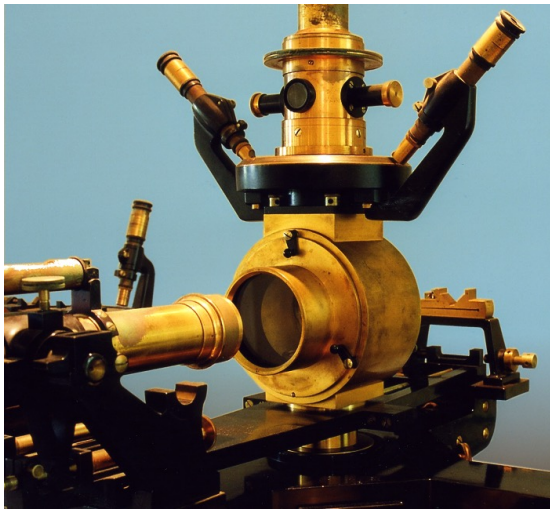

$$V = R_E \sum_{n=1}^{N} \left( \frac{R_E}{r} \right)^{n+1} \sum_{m=0}^{n} \left( g_n^m \cos m\lambda + h_n^m \sin m\lambda \right) P_n^m (\sin \beta)$$

$$\vec{B} = -\nabla V$$

$r$: radial distance
$\lambda$, $\beta$: Longitude, Latitude
$R_E$: Earth's radius
$g_n^m$, $h_n^m$: Expansion coefficients

Gauß (1839)

## *First global map of magnetic field strength*

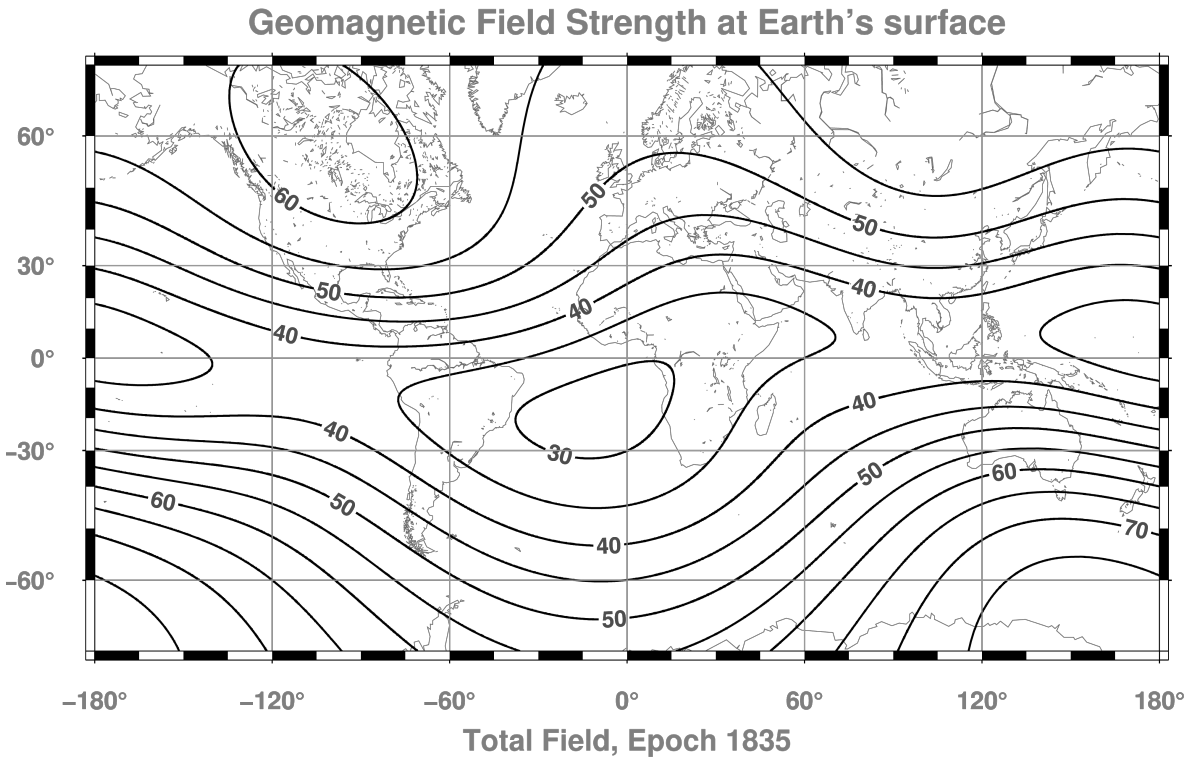


Gauß et al. (1840)

Gauß succeeded in providing a good representation of field distribution over the globe. This is the first time that the South Atlantic Anomaly is identified.

In spite of the fairly low number and uneven distribution of observatories he obtained this great result. This demonstrates the power of the spheric harmonic analysis for recovering the geomagnetic field distribution.

This is one reason why the spherical harmonic expansion is still the backbone of geomagnetic field modelling today. It furthermore allows to separate contributions from external and internal sources.

## *Satellite era, History of magnetic field missions*

### Magsat

First vector magnetic field satellite
(1980, 6 months) dawn-dusk

### Ørsted

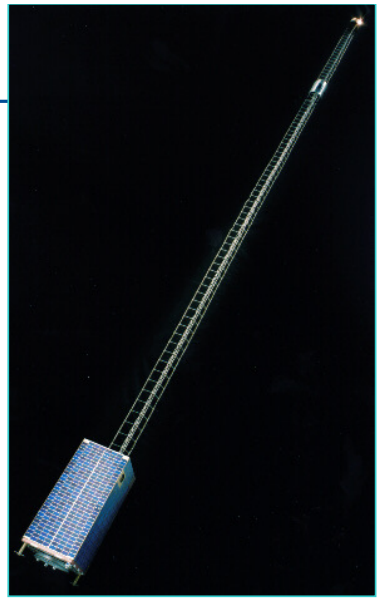

Mission: Feb 1999 - 2004
Polar orbit, 650-850 km altitude
Quasi sun-synchronous
(all local times within 2.2 years)

### CHAMP

Mission: July 2000 – Sep. 2010
Low altitude (450 – 300 km)
All local times within 130 days

### Swarm

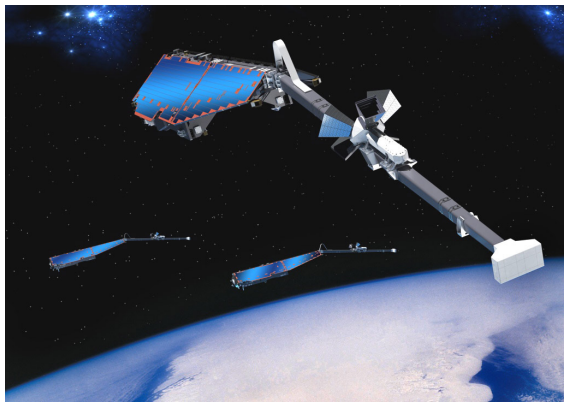

Mission: 2014 – present
Three identical spacecraft
Near-polar orbits, 450 & 510 km
All local times within 135 days

## *CHAMP and Swarm, altitude evolution*

CHAMP
2000-2010

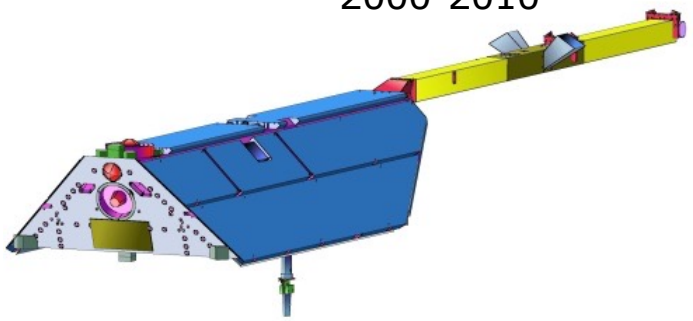

3 Swarm spacecraft
2014-present

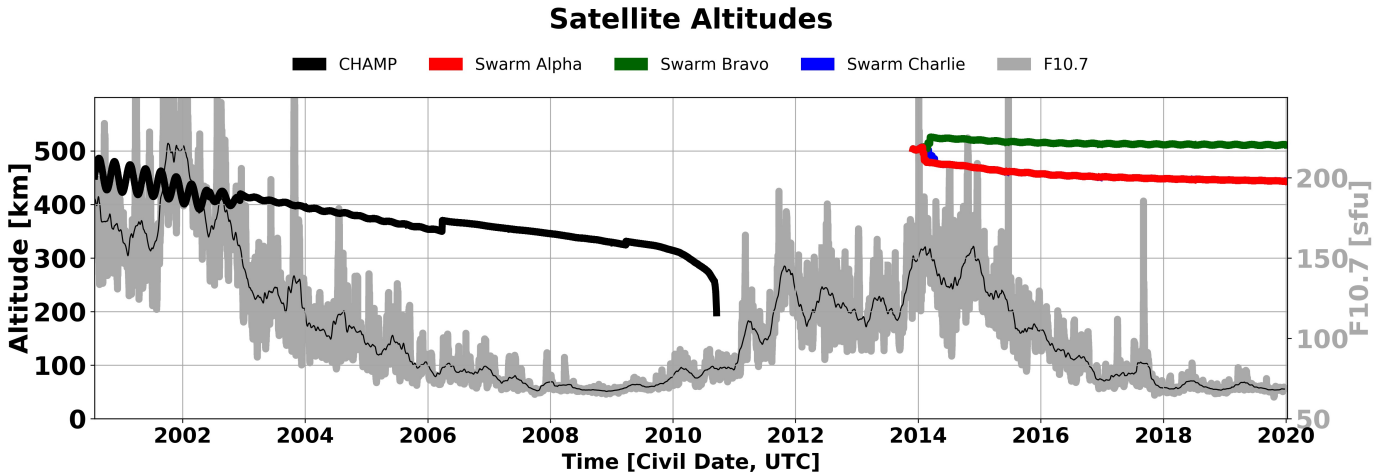


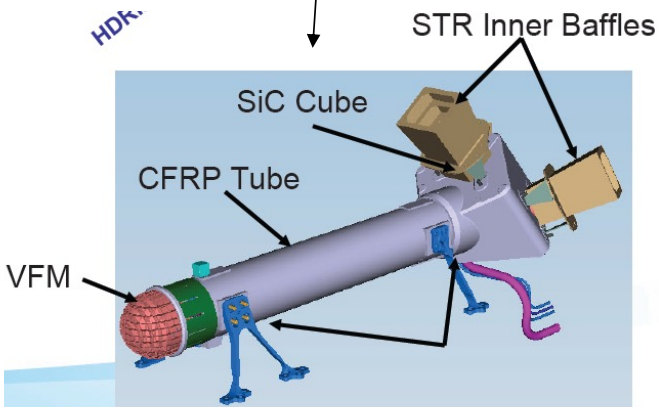

## *Satellite era, global coverage*

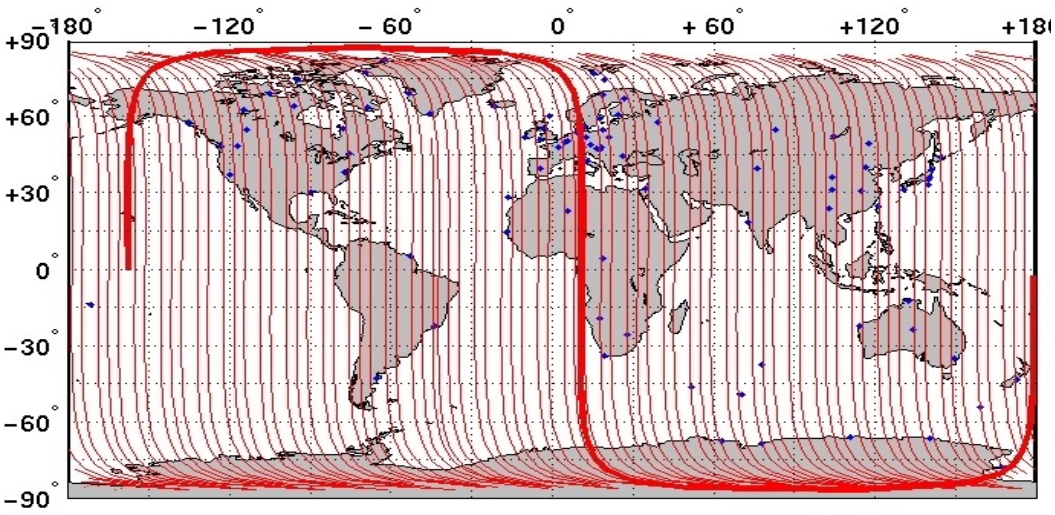


Distribution of Swarm orbits within 5 days. A good coverage is acquired within short time for a high-resolution modelling.

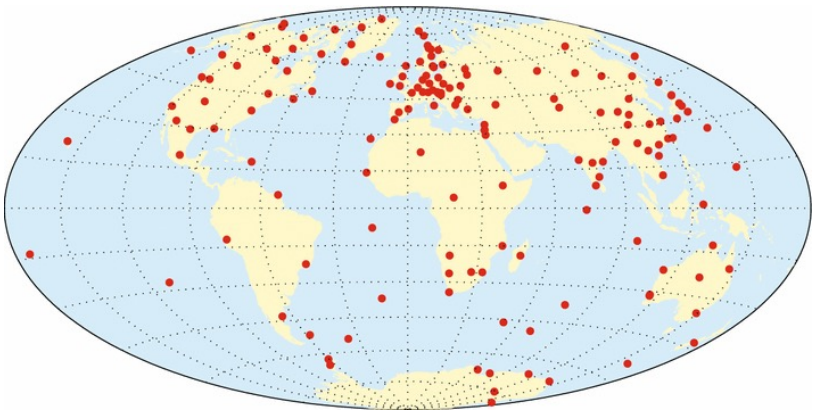

Distribution of about 100 INTERMAG ground observatories. Sparse coverage over Pacific Ocean.
Measurements are valuable additions to satellite data for characterising the temporal variations.

# *Recent geomagnetic field model*

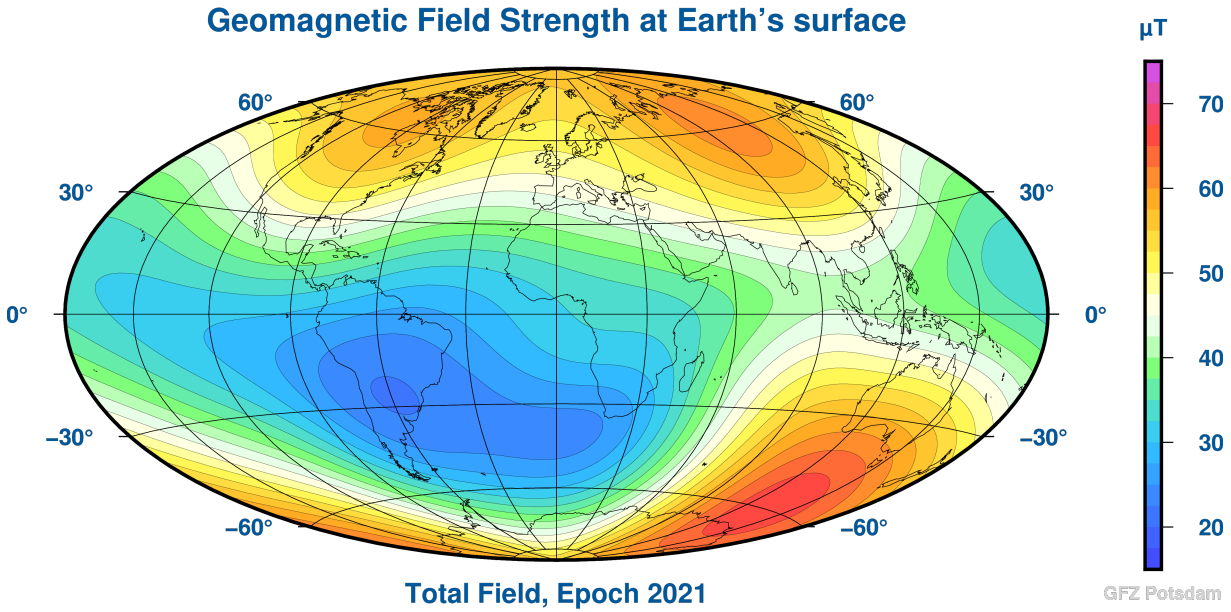


Highly precise geomagnetic field models can be derived from the combined satellite/ground-based measurements. These have to be updated about every 6 months for maintaining the precision.

Still, gross features have remained since the Gauß model.

The signal power drops off rapidly towards higher harmonics. The dipole dominates. Higher terms follow a power-law decay.

For harmonics greater than16 a white spectrum appears, reflecting signals from crustal magnetisation.

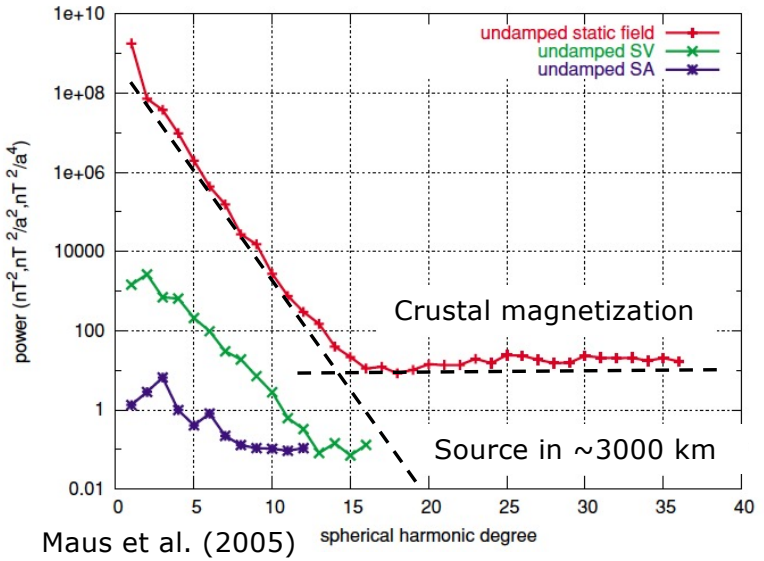


Maus et al. (2005)

# *Recent geomagnetic field model*

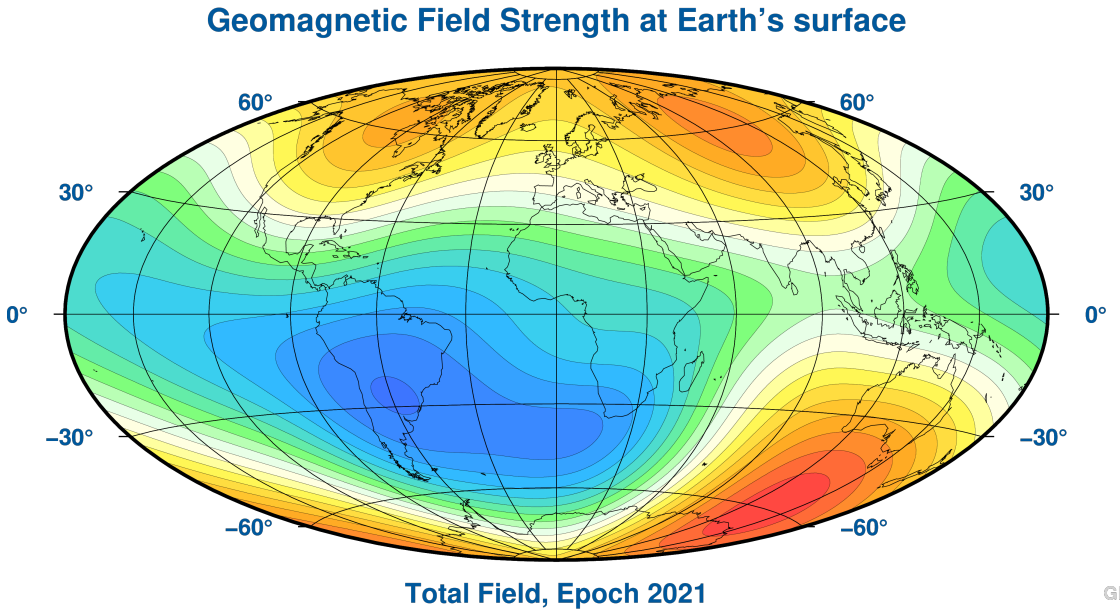


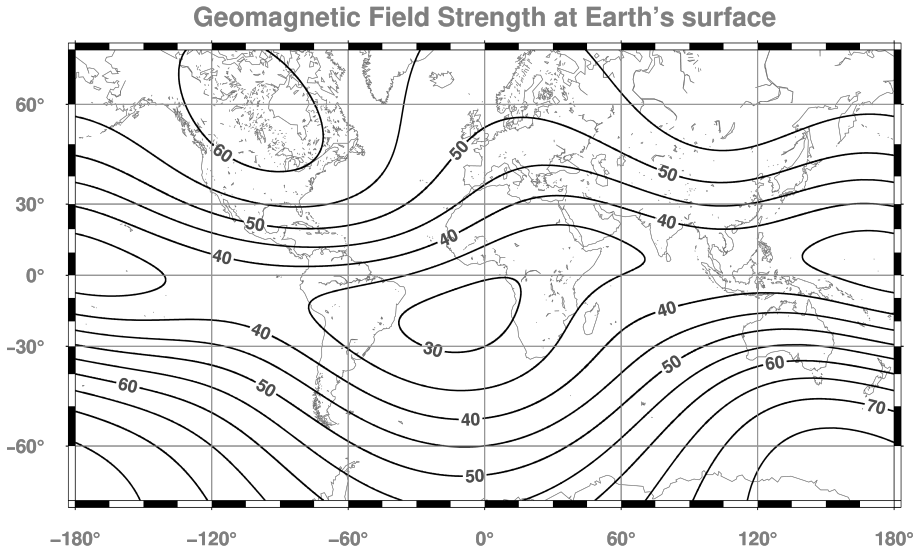


Highly precise geomagnetic field models can be derived from the combined satellite/ground-based measurements. These have to be updated about every 6 months for maintaining the precision.

Still, gross features have remained since the Gauß model.

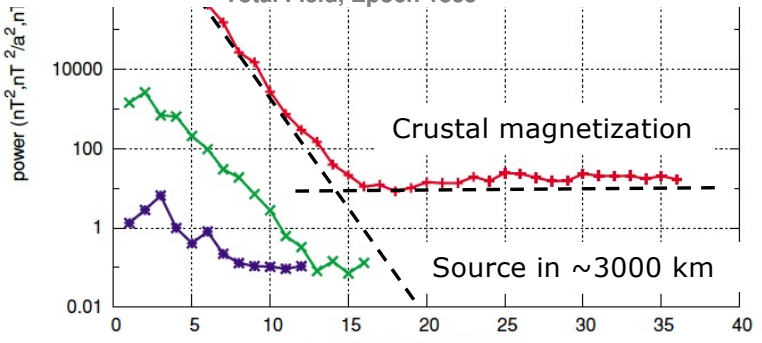


Maus et al. (2005)

## *Distribution of field changes during the past 40 years*

Changes of field strength are not evenly distributed. Over the Eurasian continent we find a slide increase. But over most other areas it decreases. Particularly strong over the Americas and South Atlantic.

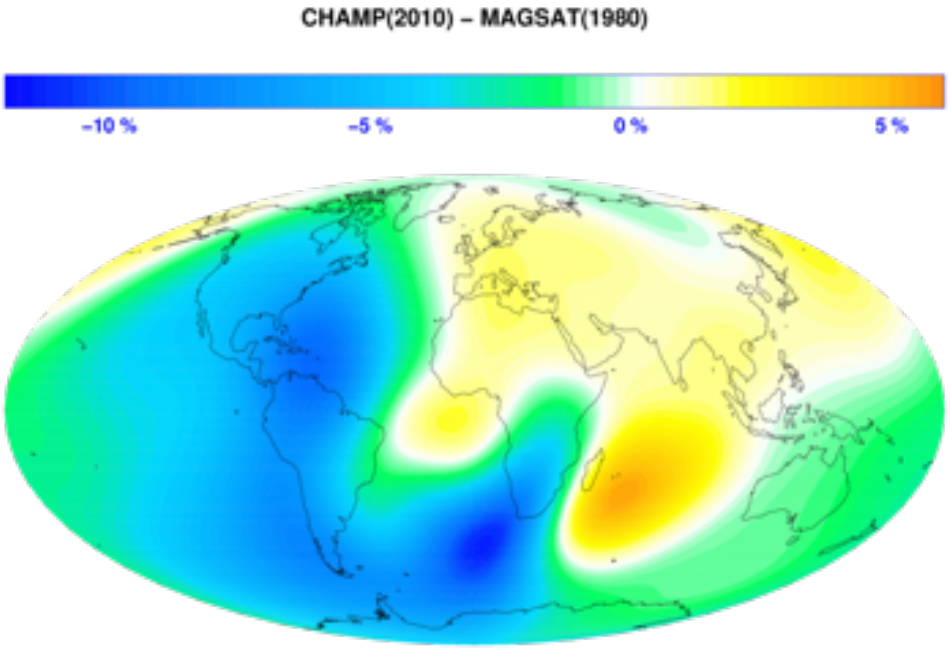


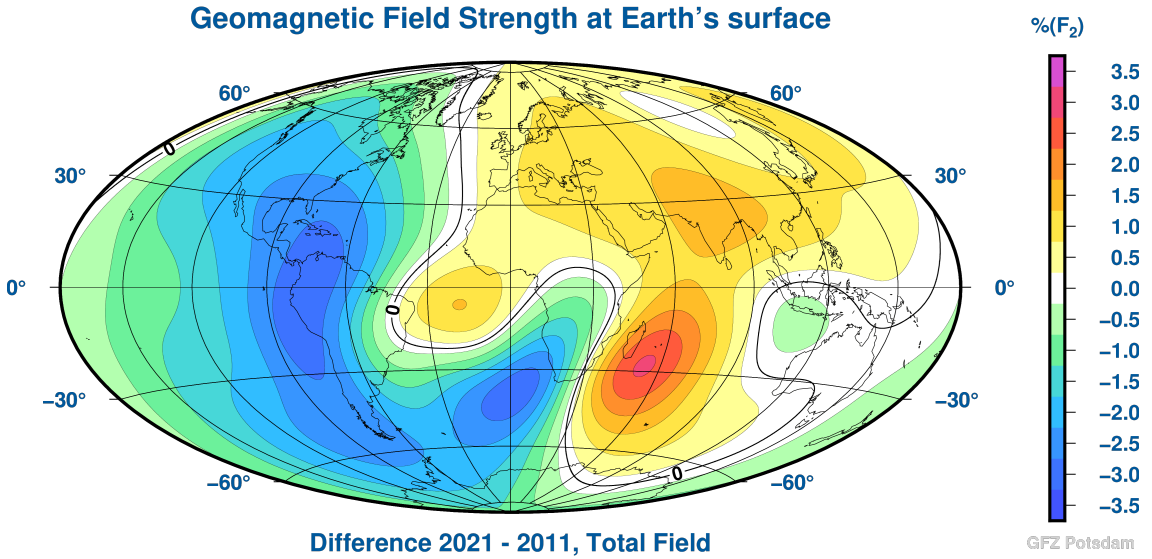


In regions of lowest field strength we find a most rapid decrease (South America/Atlantic).
Here the field weakens at a rate of 3.5% per 10 years.
This is 7 times faster than the dipole decay.
→ The South Atlantic Anomaly is deepening rapidly.

## *Radiation effects in the South Atlantic Anomaly (SAA)*

The geomagnetic field acts as a shield against adverse radiation from space. This effect is much reduced in the area of the SAA. At an altitude of 500 km the radiation from space is enhanced by a factor of 100 in the core region.

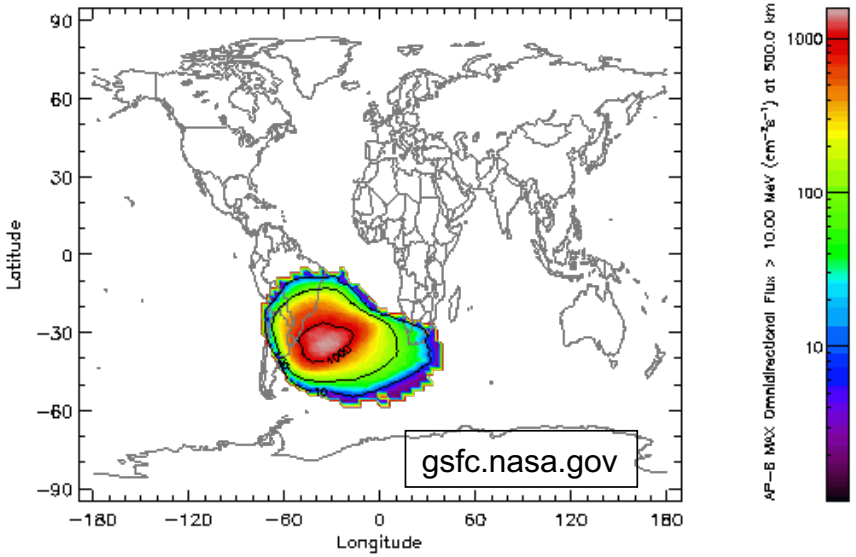


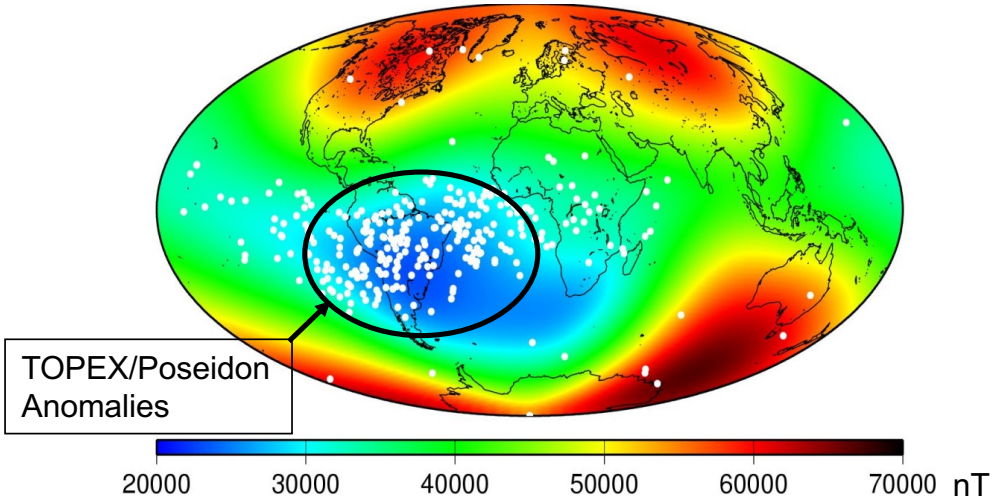


Heitzler et al. (2002)

Satellites experience here most of their operational anomalies.

With a continuing decrease of the field strength in this area the radiation will further increase.

This has consequences for ISS astronauts and satellite operations.

## *Map of crustal magnetization from CHAMP satellite*

(Radial component)

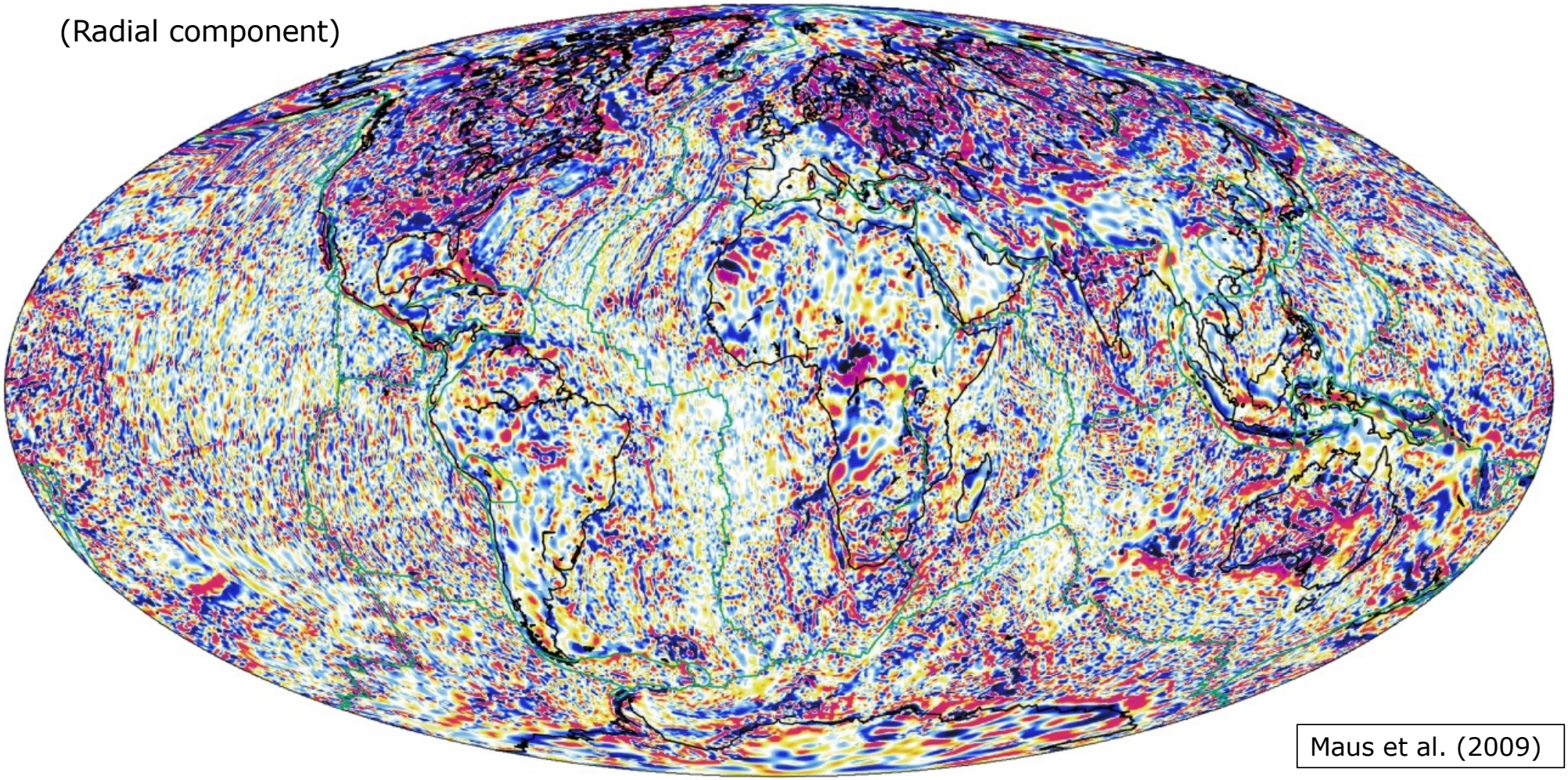

Maus et al. (2009)

## *Map of crustal magnetization from CHAMP satellite*

(Radial component)

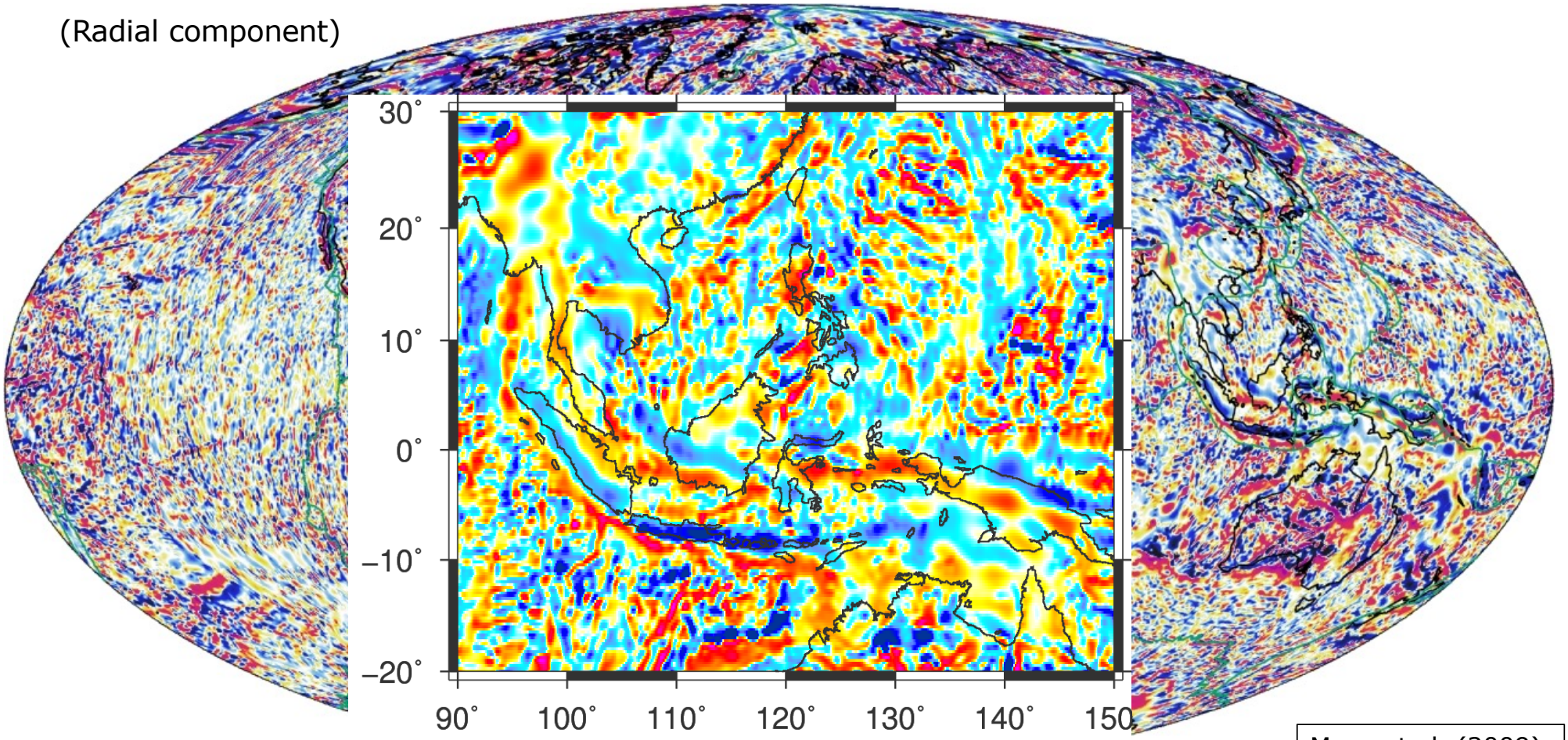


Maus et al. (2009)

## *Interpretation of residual magnetic fields*

The geomagnetic field is composed of contributions from many sources.

After more than 20 years of high-resolution magnetic field measurements models of the important contributors, core field, crustal field, and ring current are so precise that the small remaining observed deviations can reliably be used for investigating other processes.

Magnetic fields are used more and more as a remote sensing signal.

## *Magnetic signatures of ocean tides*

Ocean currents, including tides, drive salty water across the geomagnetic field. This causes electric currents that generate magnetic fields.

CHAMP was the first to detect the weak tidal signals.

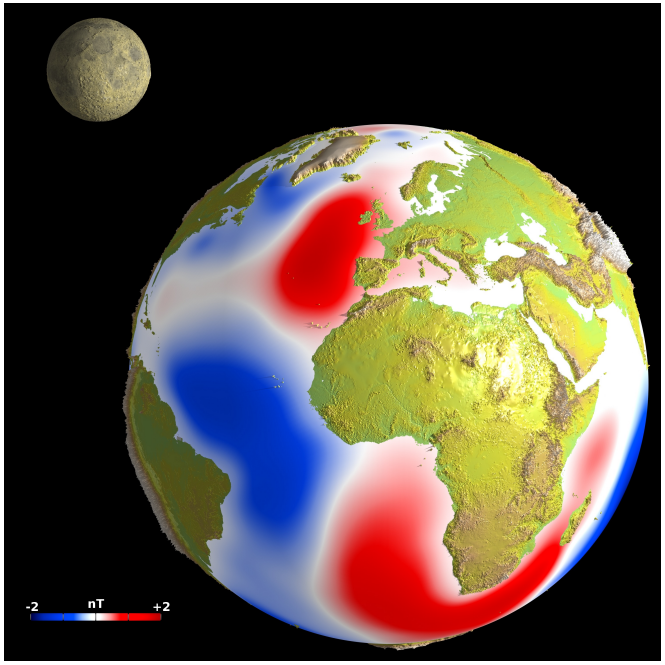


(*top frame*) Total field global pattern of ocean tides at New Moon epoch.

(*below*) Tidal prediction from ocean model.

(*lower pair*) Same as above but for 6.2 hours later.

Amplitudes range around 1 nT.

(Tyler, Maus and Lühr, Science 2003)

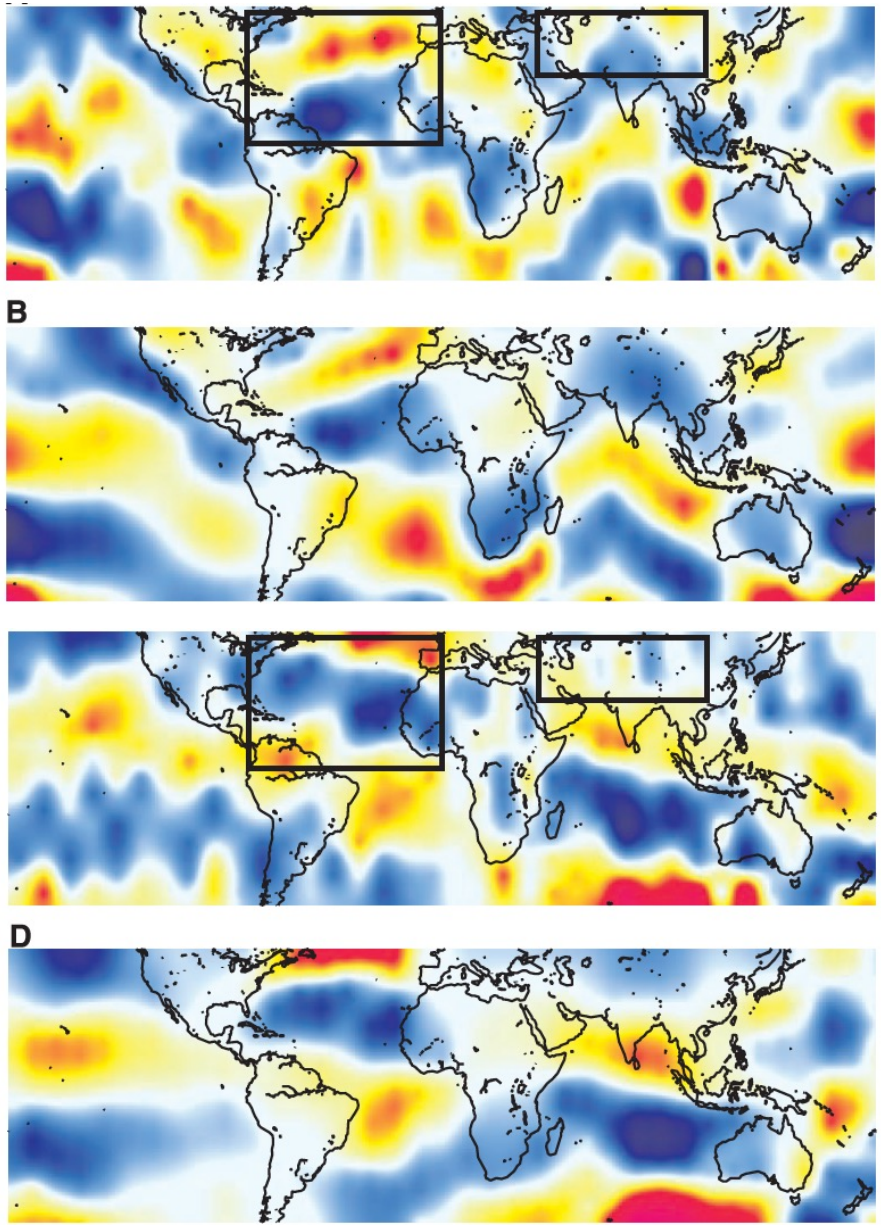

## *Magnetic signatures of ocean tides*

Ocean currents, including tides, drive salty water across the geomagnetic field. This causes electric currents that generate magnetic fields.

CHAMP was the first to detect the weak tidal signals.

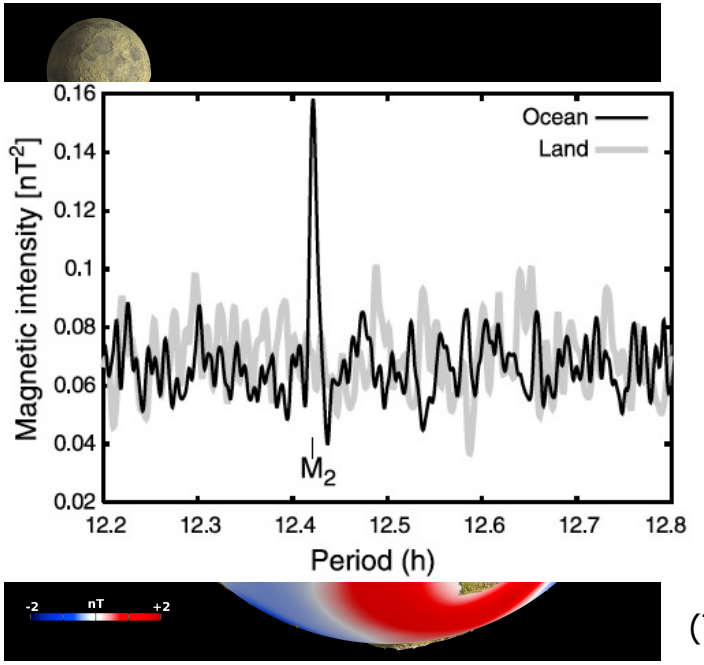


(*top frame*) Total field global pattern of ocean tides at New Moon epoch.

(*below*) Tidal prediction from ocean model.

(*lower pair*) Same as above but for 6.2 hours later.

Amplitudes range around 1 nT.

(Tyler, Maus and Lühr, Science 2003)

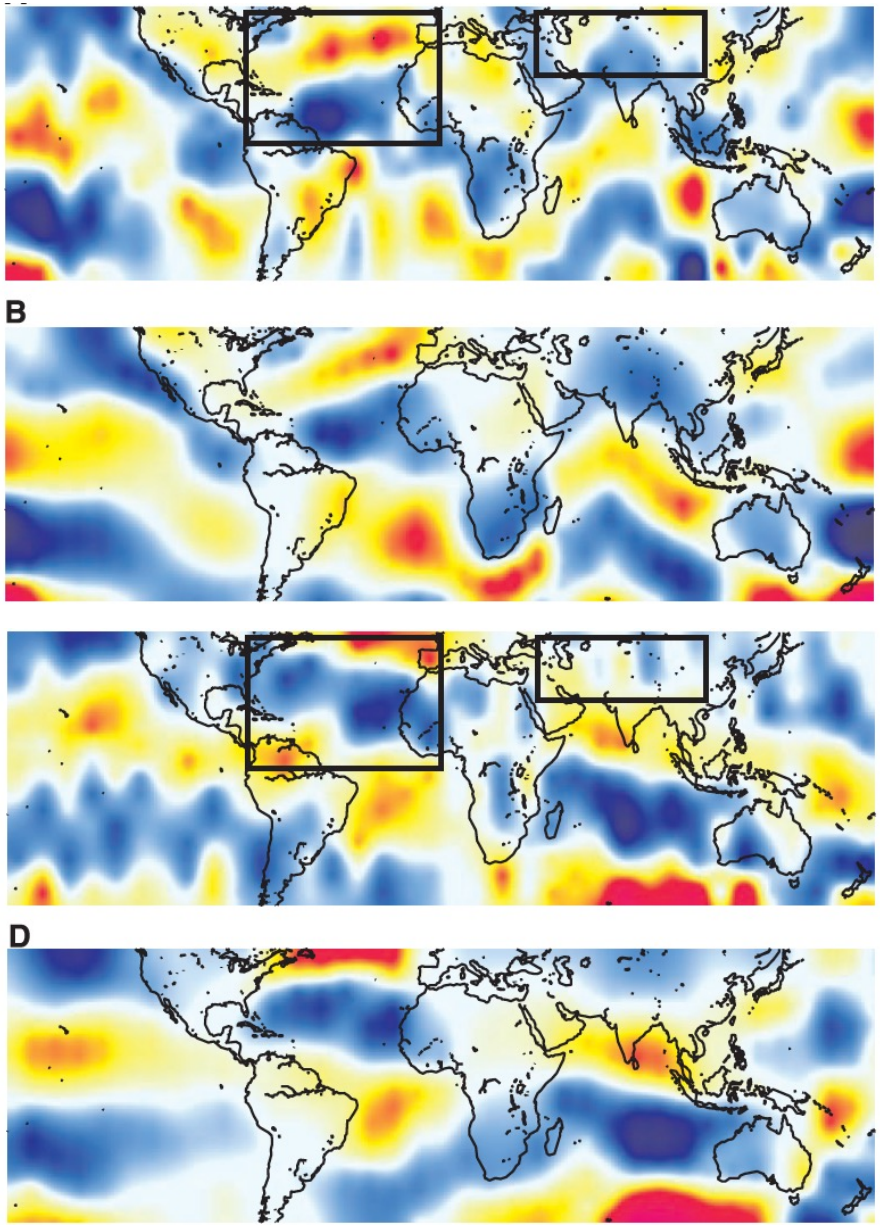

## *Magnetic signatures of ionospheric irregularities*

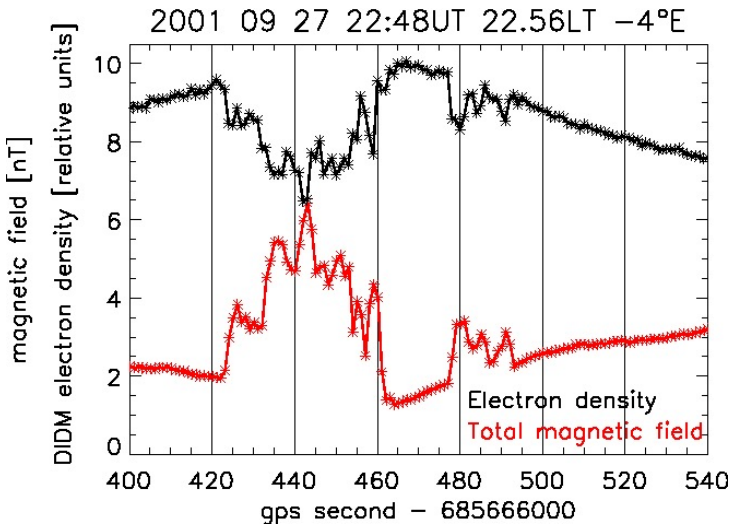


Electron density variations are closely mirrored by the magnetic field strength due to the diamagnetic effect.

$$\Delta b = -\Delta n\, k \left(T_i + T_e\right) \frac{\mu_0}{B}$$

Lühr et al. (2003)

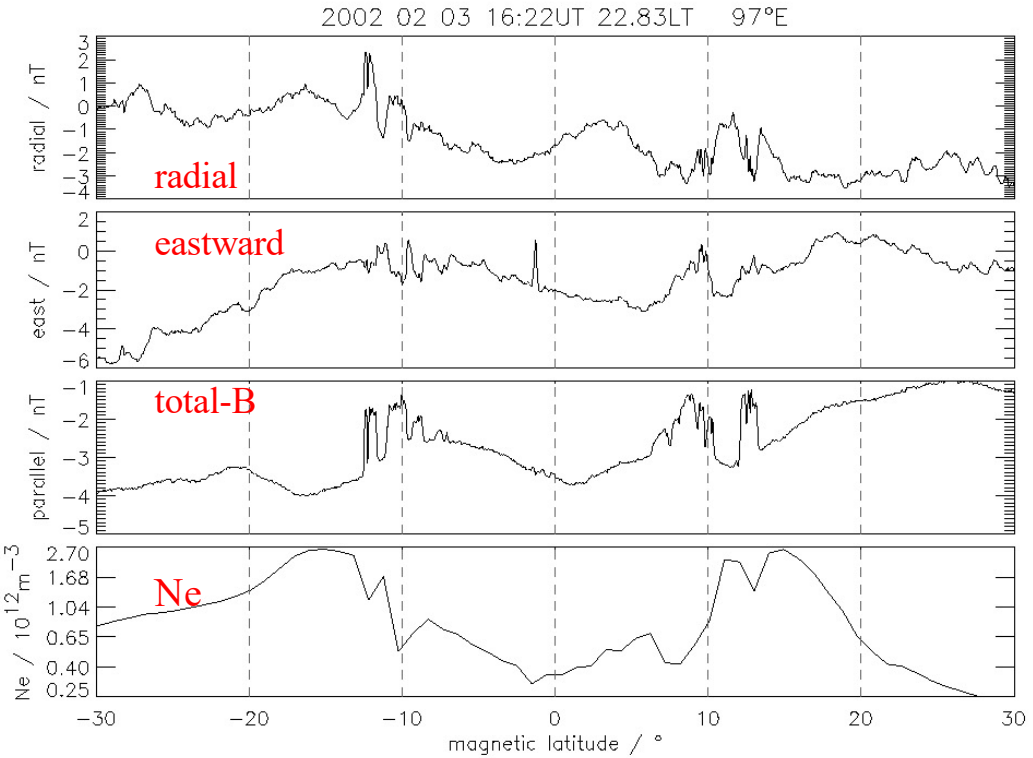


south ← north

CHAMP pass

Stolle et al., 2006, JGR

## *Seasonal variation of GPS signal disturbance*

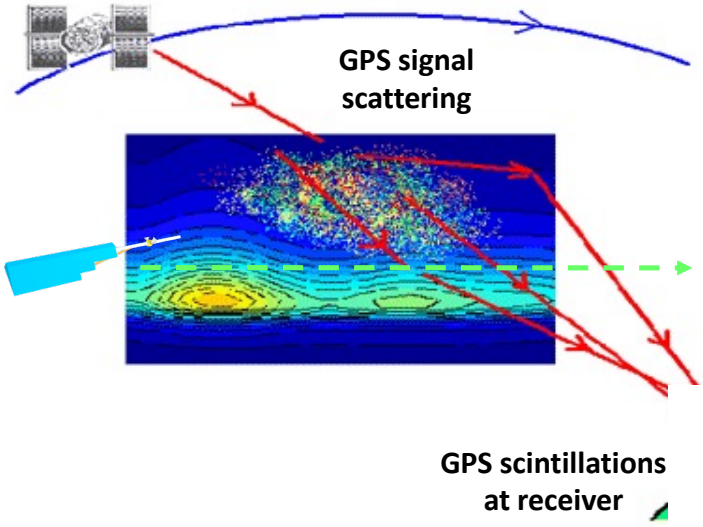


When GPS signals traverse ionospheric irregularities, they are damped and scattered.

The occurrence rate of the irregularities shows a distinct seasonal/longitudinal pattern.

(Stolle et al., 2006)

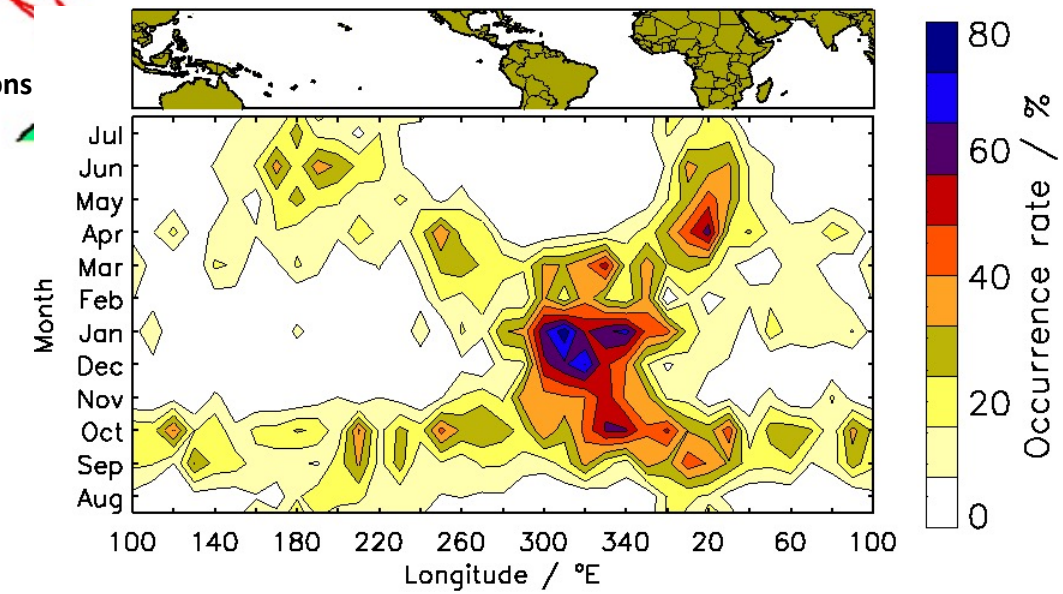

## *Probing electric currents by using Ampère's integral law*

$$\mathbf{j} = \frac{1}{\mu_0 A} \oint \mathbf{B}\, d\ell$$

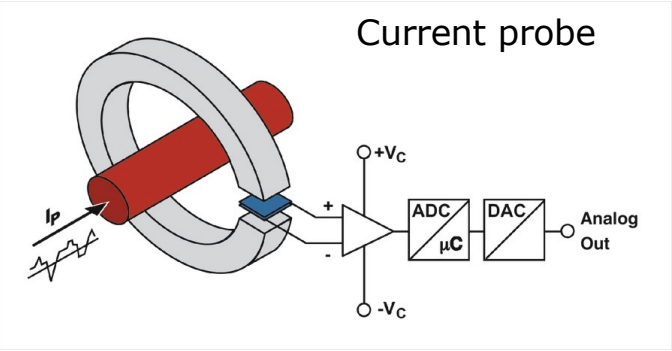


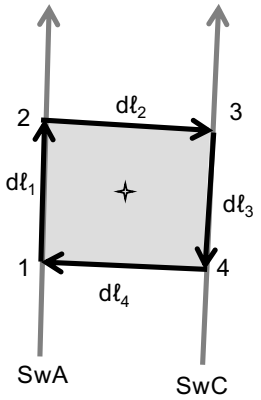


(Ritter et al., 2013, EPS)

Magnetic field data of Swarm A and C, flying side-by-side, are used for estimating current density.

Along-track variation, $B_X$, is derived from two subsequent measurements

$$dt = 5sec \rightarrow dl_{1,3} = 38km$$

Cross-track separation is 1.4° in longitude.

Vertical current, $j_Z$, is projected on the field direction, to get FAC.

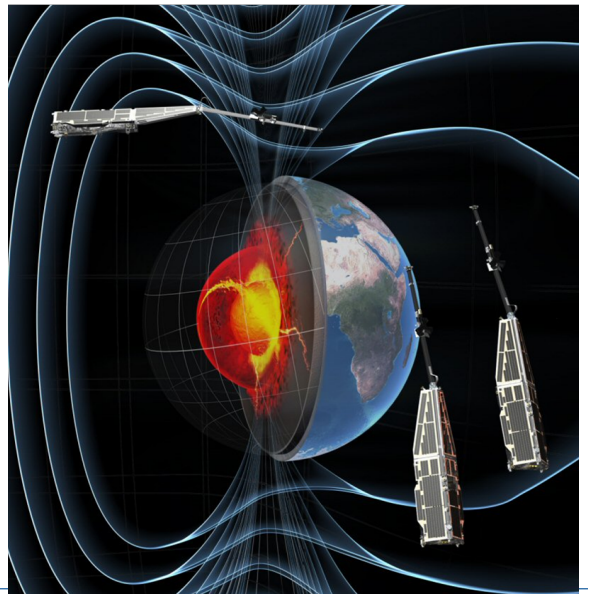

## *Ionospheric current systems*

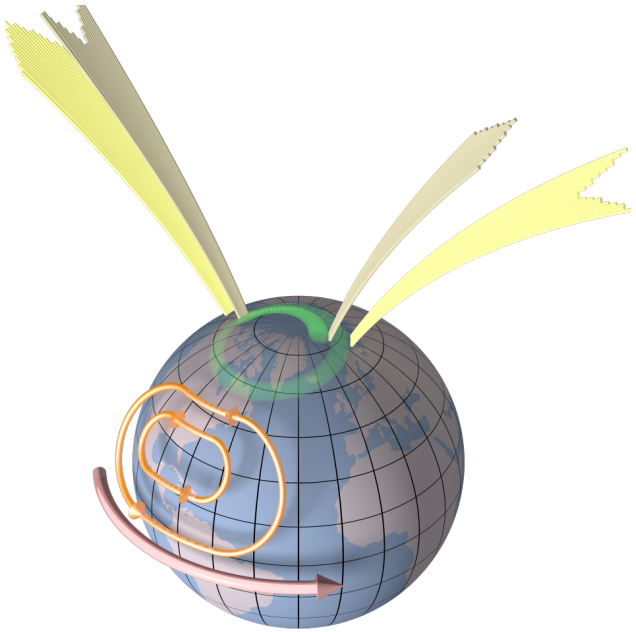

There are several current systems that can well be sensed and investigated with satellites like CHAMP and Swarm.

At high latitudes we have the auroral electrojets and the field-aligned currents, connecting to sources in the magnetosphere.

At middle latitudes the solar quiet (Sq) currents are dominating.

Above the magnetic equator the strong equatorial electrojet (EEJ) is flowing.

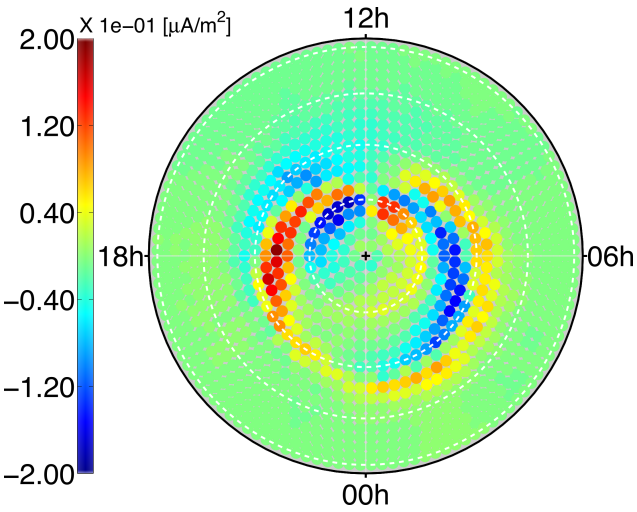


Auroral field-aligned currents
(yellow, red: upward current)

# Solar quiet (Sq) current system, seasonal variation

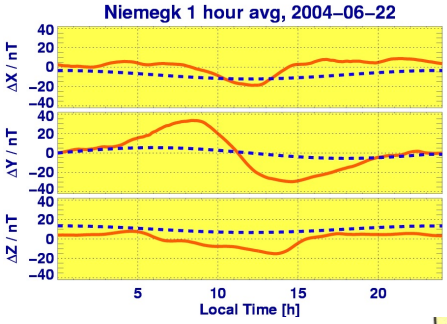


The Sq system involves current vortices in the two hemispheres.
It is limited to dayside hours and stronger in the summer hemisphere.

Having field measurements from above and below the ionosphere enables reliable current estimates on global scale.

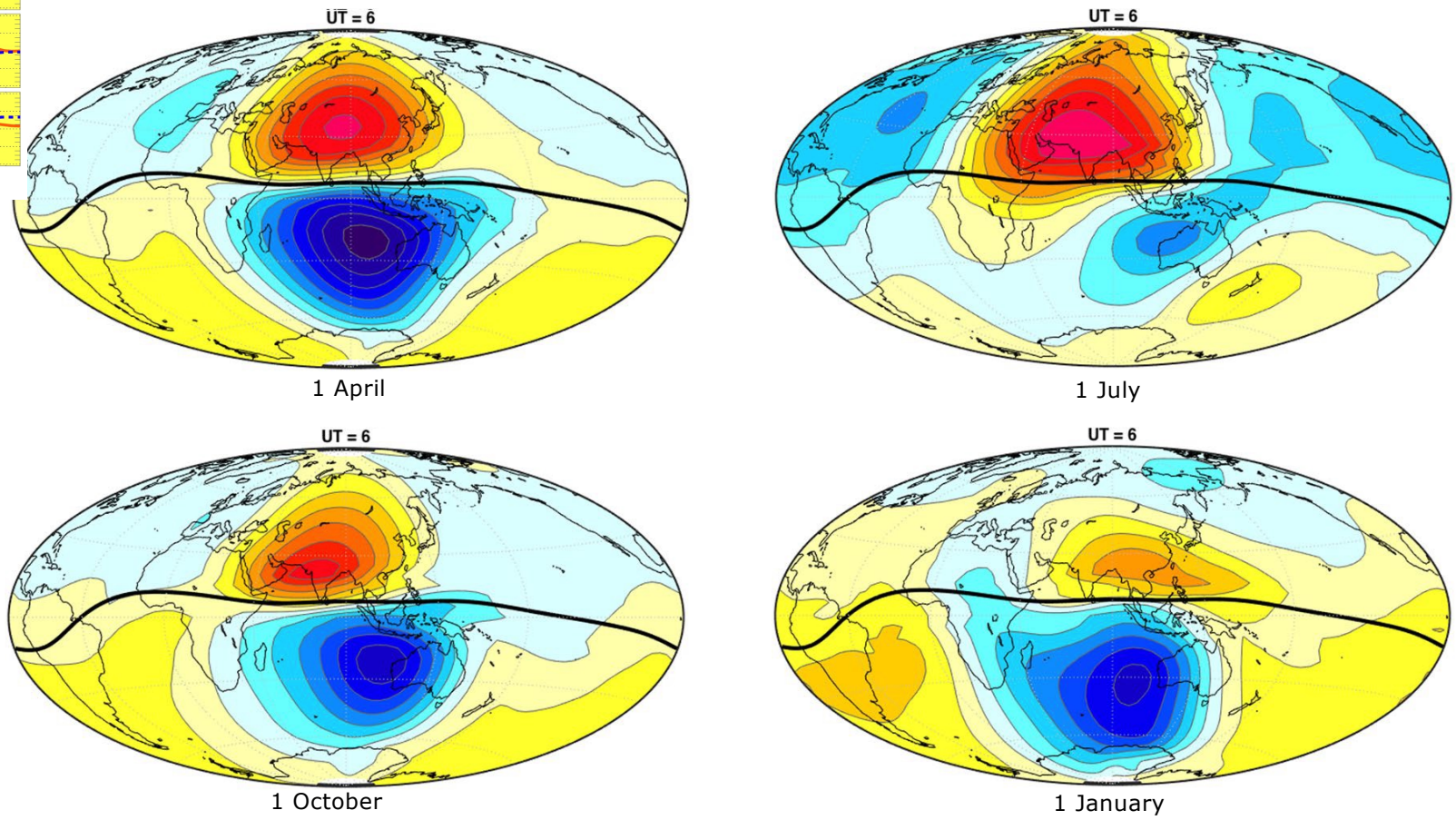


Derived from the combination of ground-based and satellite data (Chulliat et al., 2016)

# *Inter-hemispheric field-aligned currents (IHFAC) from Swarm*

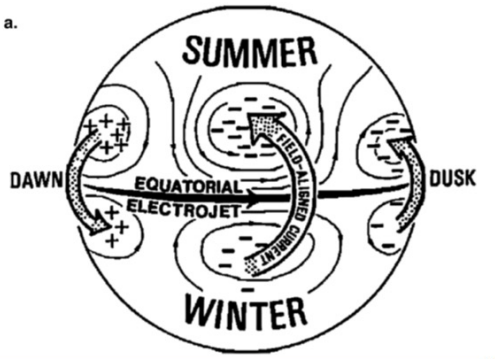


Fukushima (1994)

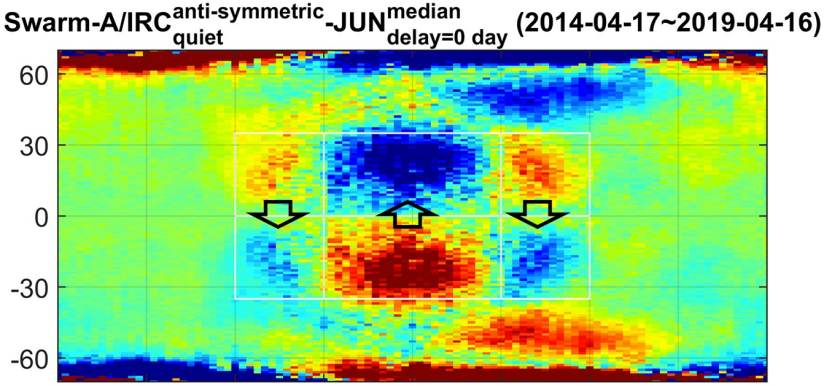


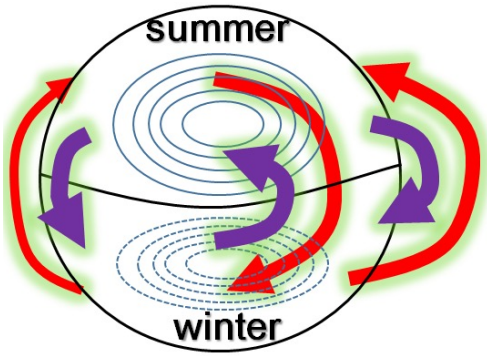


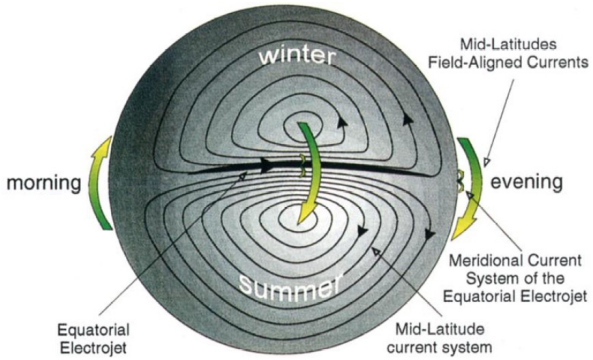


Fukushima (1979)

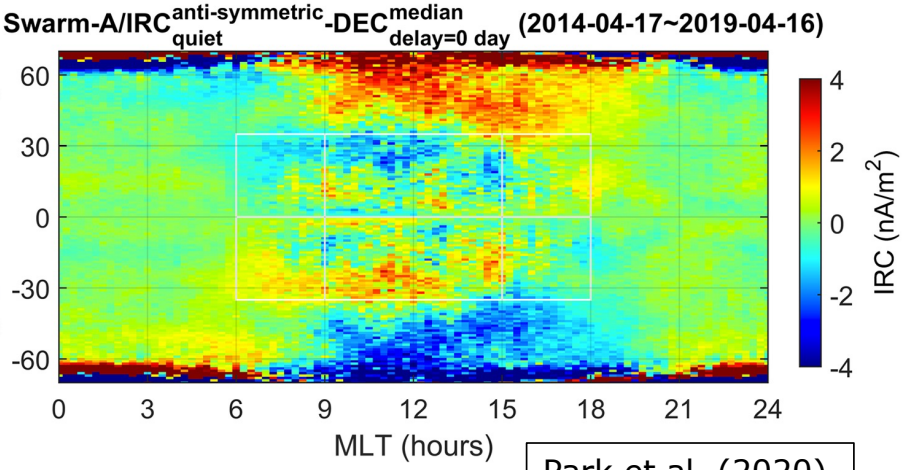


Park et al. (2020)

Earlier models predicted inter-hemispheric currents from the Sq focus in the winter hemisphere to the summer hemisphere.

For June conditions observations mainly confirm predictions, except at dusk. But the source region is south of the focus. North of 35° Lat opposite IHFACs appear.

For December conditions, opposed to predictions, no clear IHFAC patterns are observed.

# *Magnetic signature of the equatorial electrojet (EEJ) from CHAMP*

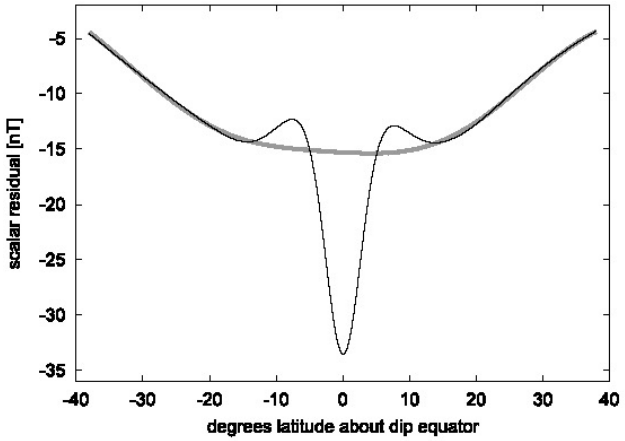


The EEJ is an intense ionospheric eastward current at the magnetic equator during daytime. It is mainly driven by the large-scale electric field, but also modulated by atmospheric tidal winds.

Satellite observations provided the first true global distribution of the current density.

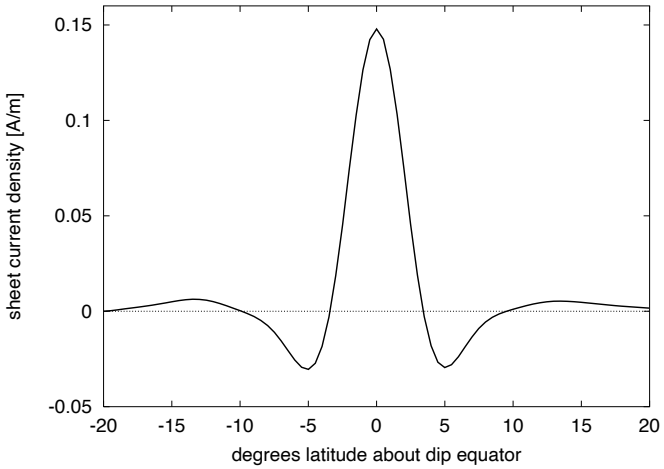


(Lühr et al., 2004)

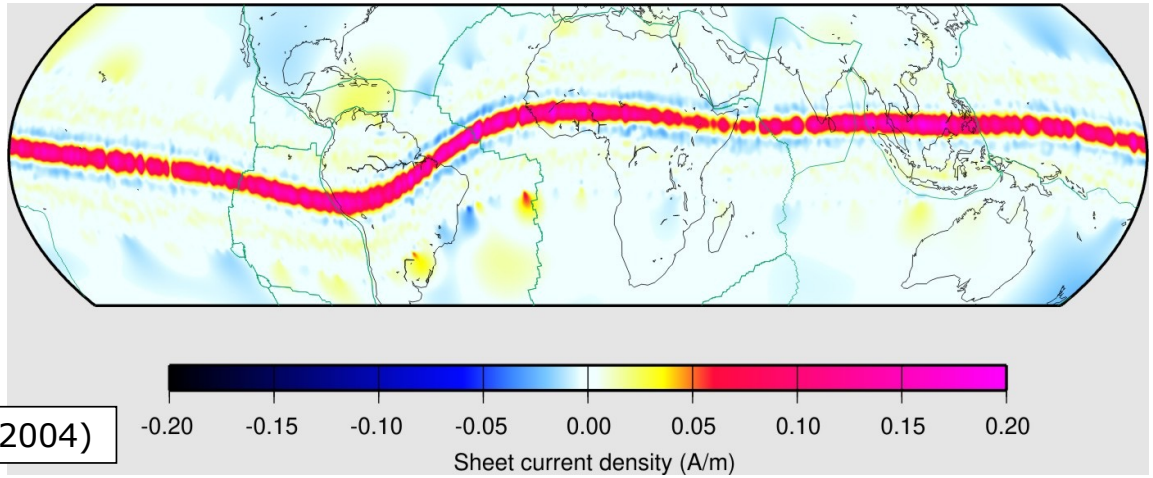

## *Longitudinal distribution of the EEJ current density (tidal signals)*

The true longitudinal distribution of the EEJ intensity was long under debate.

Only CHAMP data showed its strong seasonal dependence, and it is largely controlled by solar tidal activity.

Generally, the EEJ can be considered as a sensitive indicator for atmospheric dynamics.

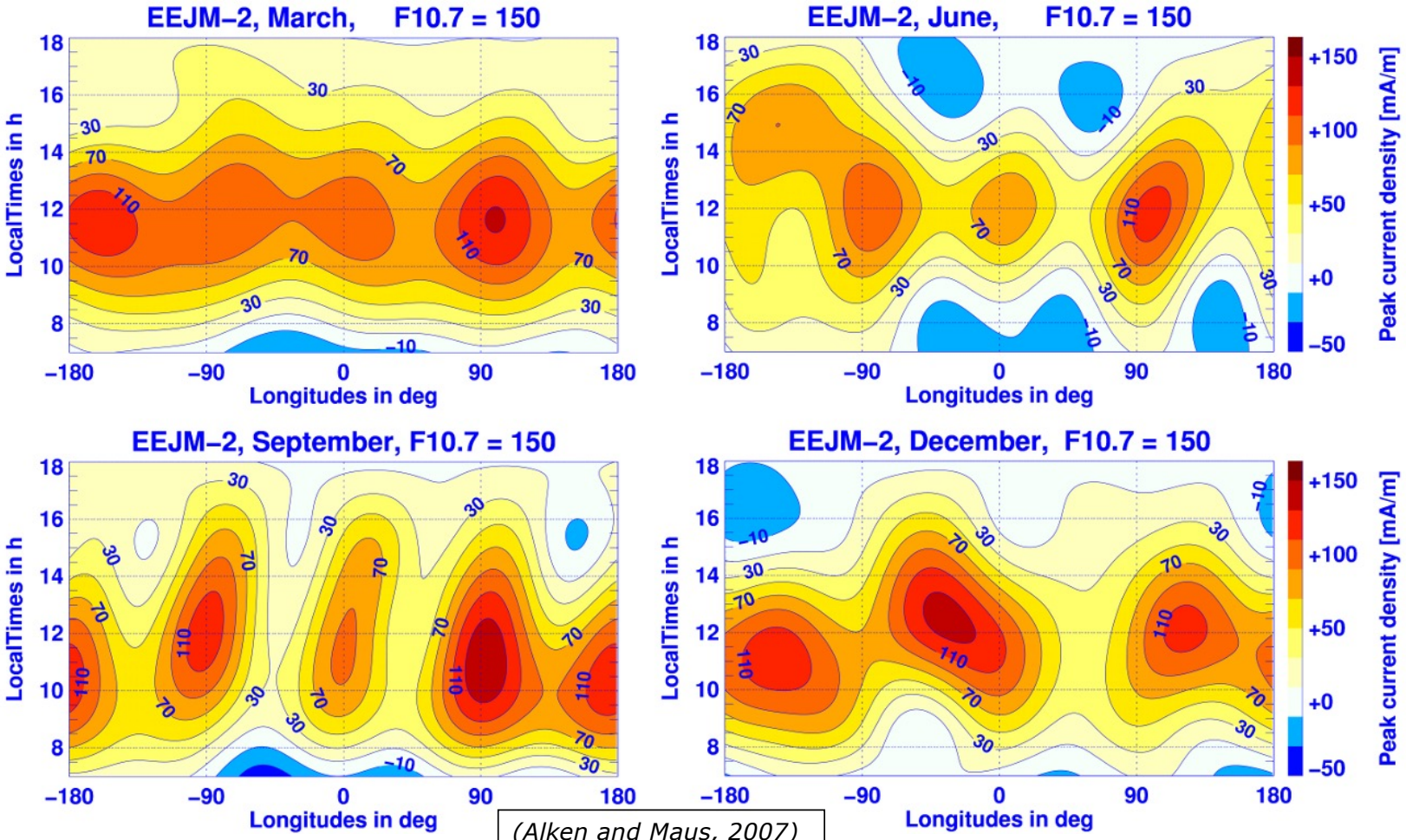


*(Alken and Maus, 2007)*

## *Cause for tidal signal in electrojet*

Tidal signals are particularly strong during autumn. These are driven by atmospheric disturbances from below.

The activity patterns are well consistent with the phase propagation of the tidal wave (DE3).

(Lühr and Manoj, 2013)

CHAMP radio occultation measurements confirm the presence of thunderstorm cells below activity maxima.

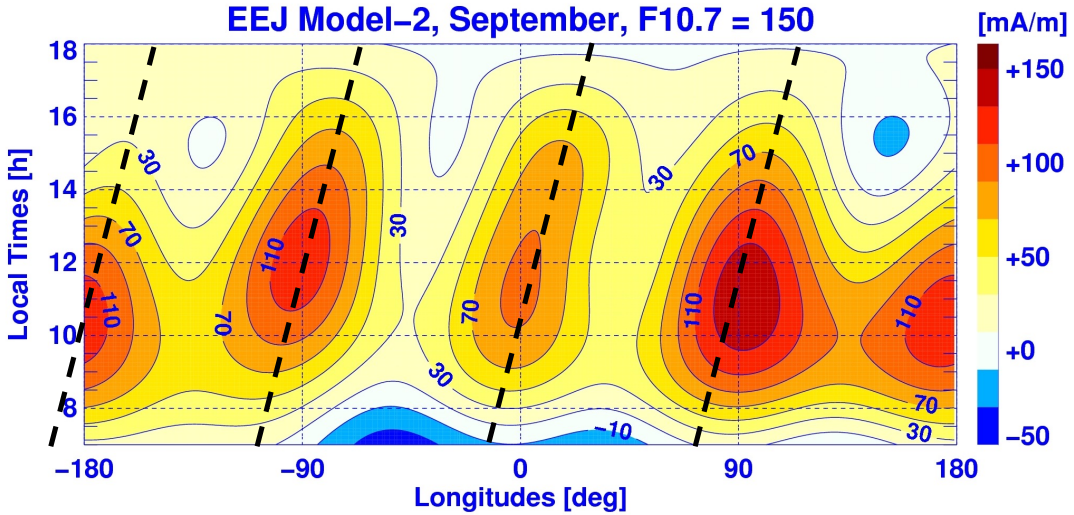


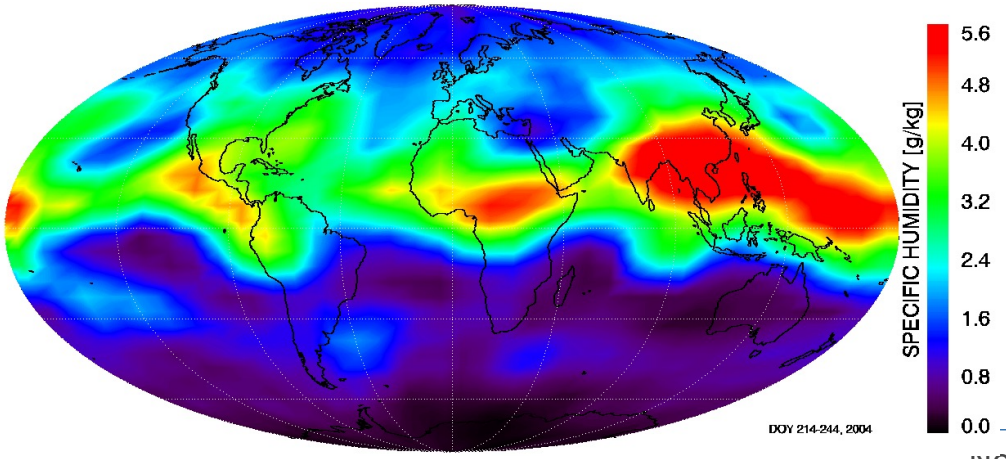

# *Polar vortex and stratospheric sudden warming (SSW)*

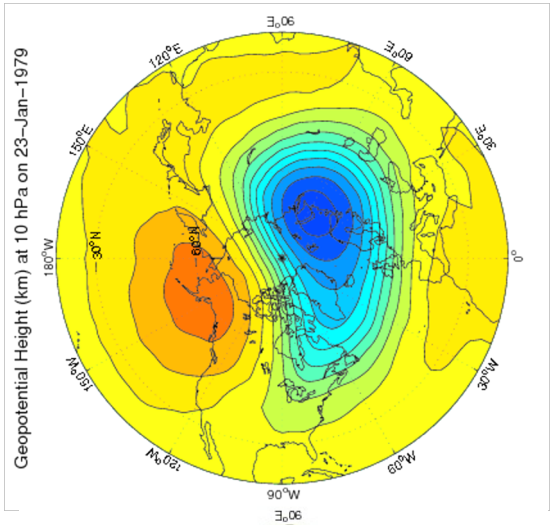


Commonly, a strong wind vortex forms over the Artic in winter enclosing very cold air.
In the 1950s it was discovered that in some years the vortex splits (Scherhag et al. 1954)

During those years (such as 2003) warm air drifts towards the pole and splits the polar vortex, pushing the cold air towards North America and Siberia. This is termed stratospheric sudden warming (SSW).

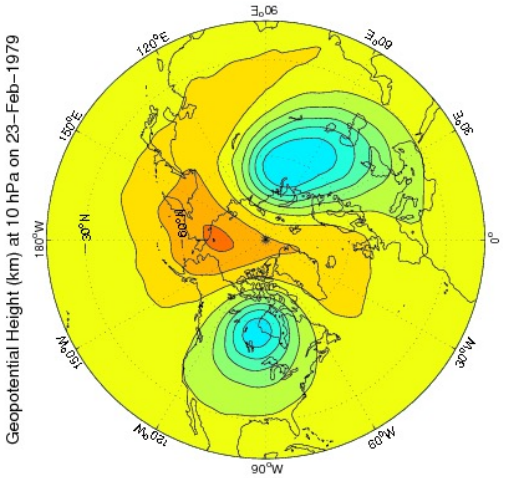


SSWs cause major reconfigurations of the upper atmospheric dynamics.
Interestingly, during the period of an SSW the modulation of the EEJ by the lunar tide is strongly enhanced.
The mechanism responsible for it is still not well understood.

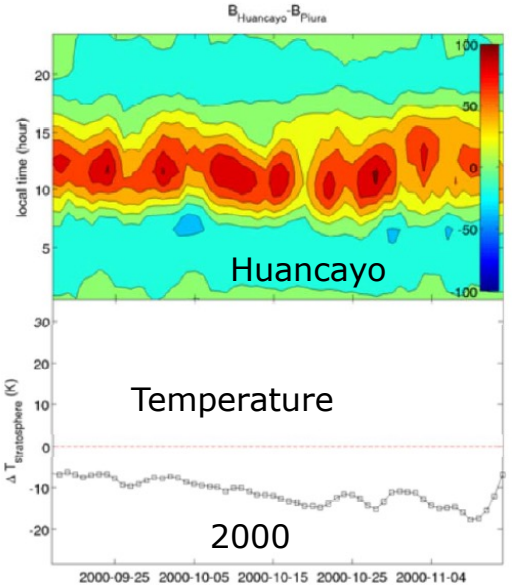


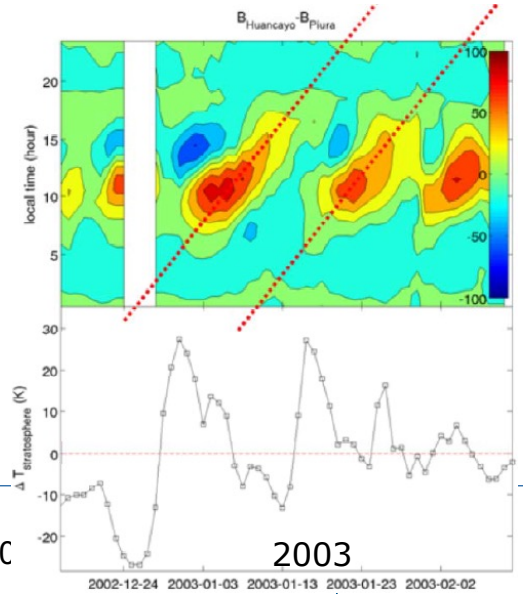

## *Lunar tide vs. SSW*

For checking the relation between SSW and lunar tides, EEJ current estimates have been derived for the whole CHAMP mission period (2001-2010). By performing a spectral analysis of the EEJ temporal variation we identified times of strong tidal signals. They correlate very well with times of sudden temperature rises at polar regions.

Thus lunar tides in EEJ can be used as marker for SSW occurrence.

(Park et al., 2012)

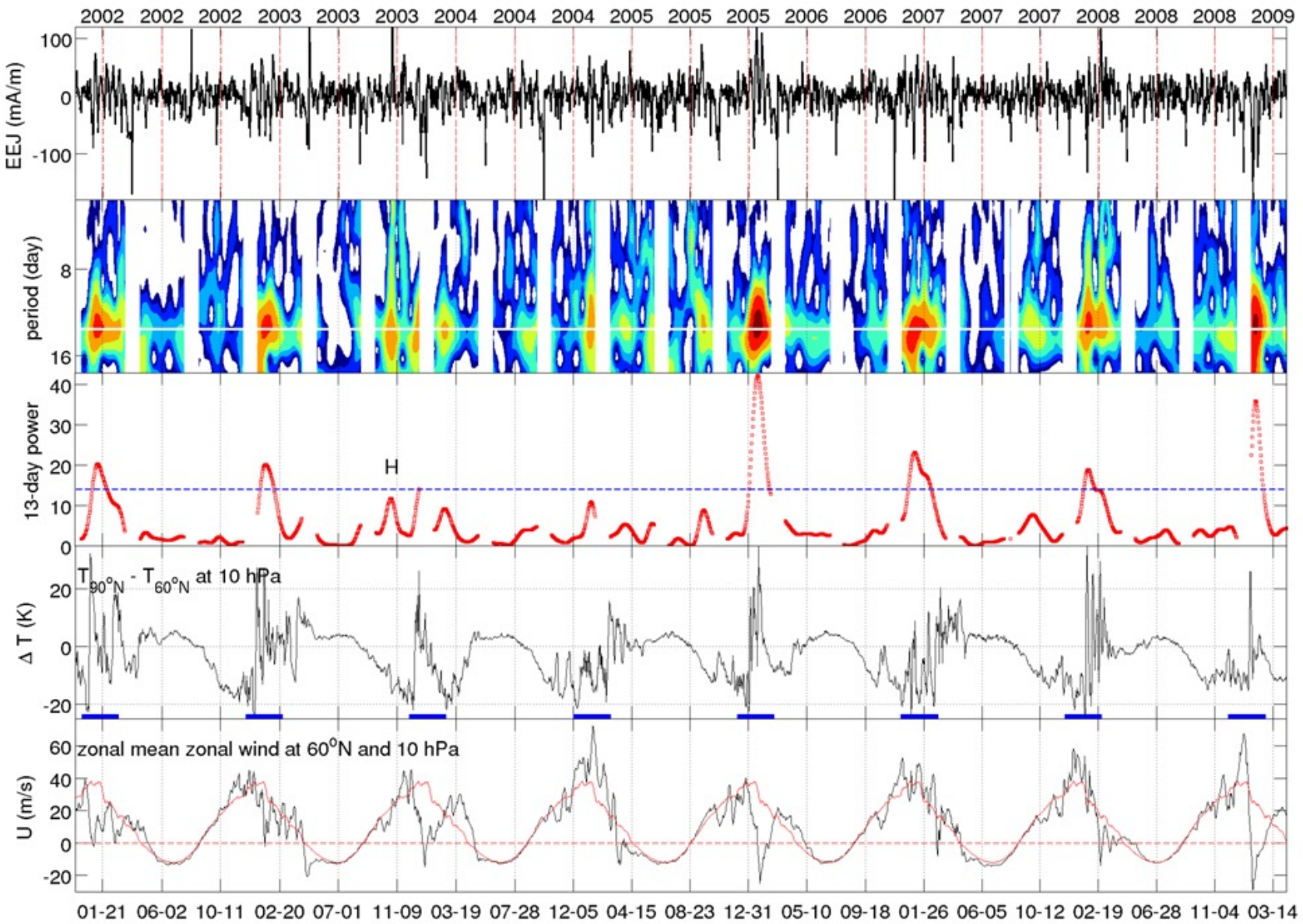


GFZ
Helmholtz-Zentrum
POTSDAM

## *Lunar tidal signal in EEJ as estimates for SSW events*

Reliable EEJ observations are available from the Huancayo observatory since the early 1920s. These have been used for calculating the tidal amplitude in EEJ.
They provide estimates of SSW events for the time before direct observation (1926-1951).
The applied threshold level is deduced from EEJ/SSW comparisons of modern times.

In this way, SSW occurrences of past times can be estimated.

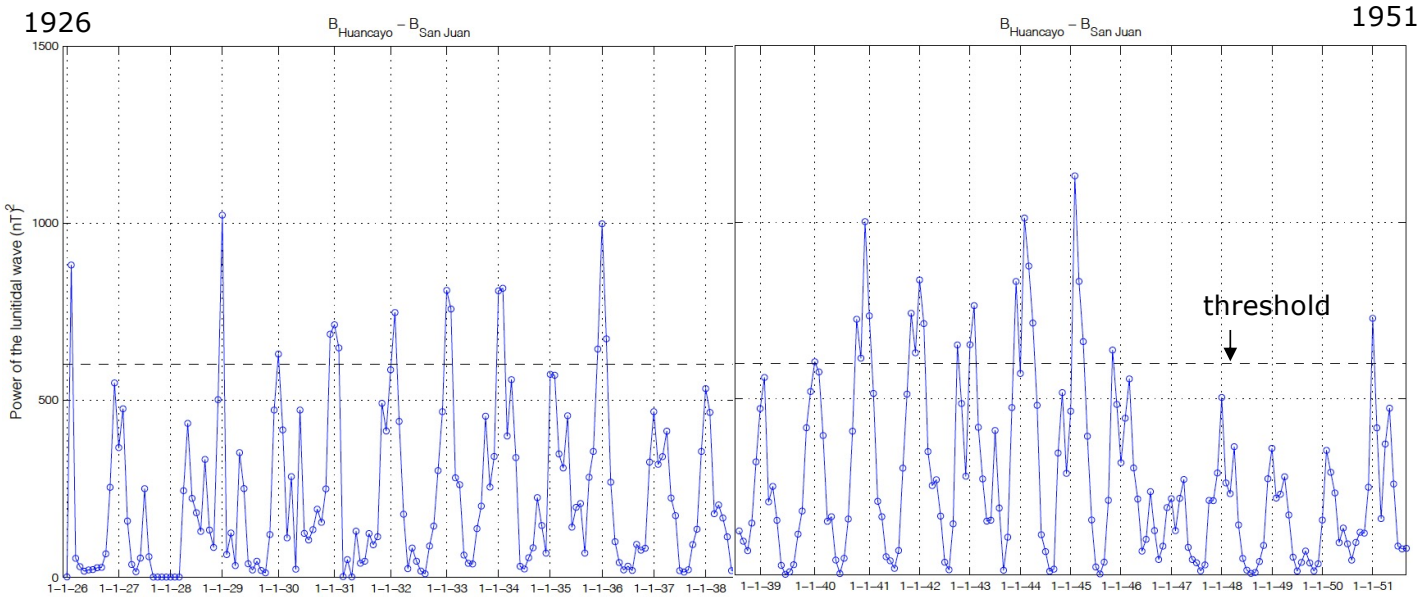


(Siddiqui et al., 2015)

## *Modulation of Sq variation by lunar tides*

During quiet days observatories at middle latitude record the typical diurnal variation (Sq system).

Also the Sq signal is modulated by the lunar tide.
Again, the tidal amplitude is largely enhanced during times of SSW occurrences. Reliable magnetic field recordings from middle latitudes are available since the 1830s. These can be used to analyse the tidal amplitude in Sq signals.

SSW events cause major changes of atmospheric dynamics. Therefore, their consideration in climate models is essential. Having a proxy for the SSW back to the pre-industrial aera is important for properly understanding past climate evolution.

Historical magnetic field recordings are probably the only candidate, which can serve this purpose of SSW spotting.

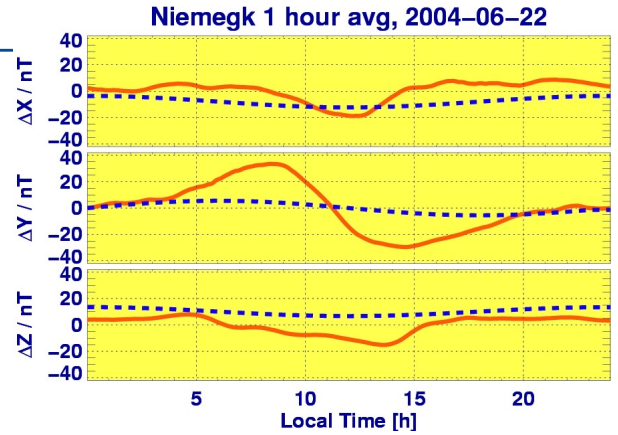


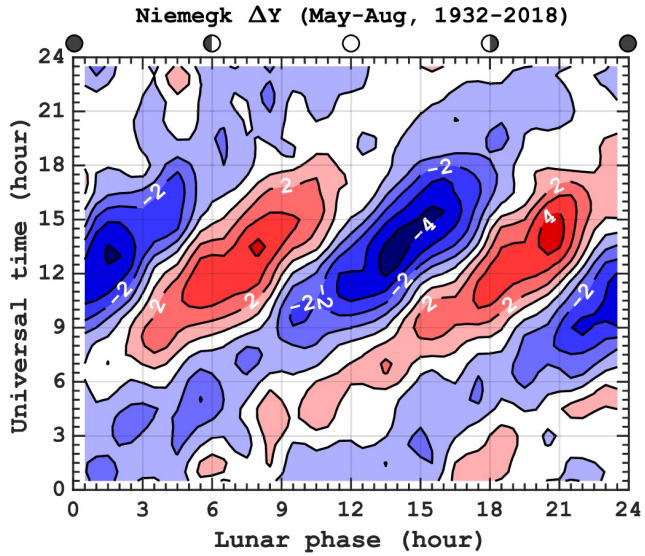

## *Summary*

- The geomagnetic field is an ever changing physical phenomena that cannot be well predicted. Therefore, continuous observations are required.
- Presently, the geomagnetic field strength is getting weaker, in particular in the South American/Atlantic region, which reduces the efficiency of shielding against adverse radiation from space.
- Satellite measurements have significantly improved the quality of main field modelling. But field contributions from other sources limit the resolution.
- This “noise component” contains a lot of information about processes in the ocean, the ionosphere, and the atmosphere.
- Historical magnetic field recordings can even make contributions to the reconstruction of past climate evolution.

## References


Alken, P., and S. Maus (2007), Spatio-temporal characterization of the equatorial electrojet from CHAMP, Ørsted, and SAC-C satellite magnetic measurements, J. Geophys. Res., 112, A09305, doi:10.1029/2007JA012524.

Brown, M., M. Korte, R. Holme, I. Wardinski, and S. Gunnarsona (2018), Earth's magnetic field is probably not reversing, PNAS, 115, 5111–5116. www.pnas.org/cgi/doi/10.1073/pnas.1722110115

Cande, S. C. and D. V. Kent (1995), Revised calibration of the geomagnetic polarity timescale for the Late Cretaceous and Cenozioc, J. Geophys. Res., 100, 6093-6095.

Chulliat, A., Vigneron, P., & Hulot, G. (2016). First results from the swarm dedicated ionospheric field inversion chain. Earth, Planets and Space, 68(1), 1–18. https://doi.org/10.1186/s40623-016-0481-6

Fukushima, N (1994), Some topics and historical episodes in geomagnetism and aeronomy, J. Geophys. Res., 99, A10, 19,113-19,142

Fukushima, N. (1979), Electric potential difference between conjugate points in middle latitudes caused by asymmetric dynamo in the ionosphere, J. Geomagn. Geoelectr., 31, 401–409.

Gauß, C. F. (1839), Allgemeine Theorie des Erdmagnetismus, in *Resultate aus den Beobachtungen des Magnetischen Verein im Jahre 1838*, pp. 1-52, Göttinger Magnetischer Verein, Leipzig.

Gauß, C. F., W. Weber, C. Goldschmidt (1840), Atlas des Erdmagnetismus nach den Elementen der Theorie entworfen, Supplement zu den Resultaten aus den Beobachtungen des Magnetischen Vereins, Weidmann, Leipzig.

Guyodo, Y. & J.-P. Valet (1999), Global changes in intensity of the Earth's magnetic field during the past 800 kyr, NATURE, 399, 249-252.

Heitzler, J.R., J.H. Allen, and D.C. Wilkinson, Ever-present South Atlantic Anomaly damages spacecraft, EOS, Trans. AGU, 83, 165, 2002.

Knudsen, M. F., P. Riisager, F. Donadini, I. Snowball, R. Muscheler, K. Korhonen, L. J. Pesonen, and B. H. Jacobsen, Variations in the geomagnetic dipole moment during the Holocene and the past 50 kyr, Earth Planet. Sci. Lett., 272, 319–329, 2008.

Korte, M. and R. Muscheler, (2012), Centennial to millennial geomagnetic field variations, J. Space Weather Space Clim. 2, A08, p1-8, DOI:10.1051/swsc/2012006

## *References*


Lühr, H., S. Maus, and M. Rother (2004), The noon-time equatorial electrojet, its spatial features as determined by the CHAMP satellite, J. Geophys. Res., 109, A01306, doi:10.1029/2002JA009656.

Lühr, H. and C. Manoj (2013), The complete spectrum of the equatorial electrojet related to solar tides: CHAMP observations, Ann. Geophys., 31, 1315–1331, doi:10.5194/angeo-31-1315-2013.

Maus, S., S. McLean, D. Dater, H. Lühr, M. Rother, W. Mai, and S. Choi, NGDC/GFZ candidate models for the 10th generation International Geomagnetic Reference Field, *Earth Planets Space*, 57, 1151-1156, 2005.

Maus, S., et al. (2009), EMAG2: A 2-arc-minute resolution Earth Magnetic Anomaly Grid compiled from satellite, airborne and marine magnetic measurements, Geochem. Geophys. Geosyst., 10, Q08005, doi:10.1029/2009GC002471.

Park, J., H. Lühr, M. Kunze, B. G. Fejer, and K. W. Min (2012), Effect of sudden stratospheric warming on lunar tidal modulation of the equatorial electrojet, J. Geophys. Res., 117, A03306, doi:10.1029/2011JA017351.

Park, J., Yamazaki, Y., & Lühr, H. (2020). Latitude dependence of inter-hemispheric field-aligned currents (IHFACs) as observed by the Swarm constellation. J. Geophys. Res.: Space Physics, 125, e2019JA027694. https://doi.org/10.1029/2019JA027694

Ritter, P., H. Lühr and J. Rauberg (2013), Determining field-aligned currents with the Swarm constellation mission*, Earth Planets Space,* 65, 1285–1294, doi:10.5047/eps.2013.09.006.

Scherhag, R.: Die explosionsartigen Stratosphärenerwärmungen des Spätwinters 1951/52, Berichte des Deutschen Wetterdienstes in der US-Zone, 6, 51–63, 1952.

Siddiqui, T., H. Lühr, C. Stolle, J. Park (2015), Relation between sudden stratospheric warming and the lunar effect on the equatorial electrojet based on Huancayo recordings, Ann. Geophys., 33, 235–243, doi:10.5194/angeo-33-235-2015.

Stolle, C., H. Lühr, M. Rother, and G. Balasis (2006), Magnetic signatures of equatorial spead-F, as observed by the CHAMP satellite, J. Geophys. Res., 111, A02304, doi:10.1029/2005JA011184.

Tyler, R.H., S. Maus and H. Lühr, Satellite observations of magnetic fields due to ocean tidal flow, SCIENCE, 299, 239-241, 2003.